(Last modified September 28, 2000)

ENCYCLOPEDIA OF VIBRATIONS

Academic Press

MS 197

ACTUATORS AND SMART STRUCTURES

Giurgiutiu, Victor

Department of Mechanical Engineering, University of South Carolina, Columbia, SC 29208, USA

Contact point: Dr. Victor Giurgiutiu
Department of Mechanical Engineering
University of South Carolina
Columbia, SC 29208, USA
803-777-8018
FAX 803-777-0106
E-mail *victorg@sc.edu*
http://www.engr.sc.edu/research/lamss/default.htm

TABLE OF CONTENTS

1 INTRODUCTION

The subject of smart structures and induced-strain actuators has attracted considerable attention in recent years. Smart structures offer the opportunity to create engineered material systems that are empowered with sensing, actuation, and artificial intelligence features. The induced-strain active materials actuators are the enabling technology that makes adaptive vibration control of smart structures realizable in an optimal way. Some generic concepts about smart structures and induced-strain active materials actuators will be given first. Then, details will be presented about piezoelectric, electrostrictive, magnetostrictive, and shape memory alloy materials that are used in the construction of induce-strain actuators. Guidelines for the effective design and construction of induced-strain actuation solutions will be provided. Details about sensory, actuatory, and adaptive smart structures will be provided, together with some real-life application examples. Conclusions and directions for further work are given last.

1.1 SMART STRUCTURES CONCEPTS

The discipline of *adaptive materials and smart structures*, recently coined as Adaptronics, is an emerging engineering field with multiple defining paradigms. However, two definitions are prevalent. The first definition is based upon a *technology paradigm:* "the integration of actuators, sensors, and controls with a material or structural component". Multifunctional elements form a complete regulator circuit resulting in a novel structure displaying reduced complexity, low weight, high functional density, as well as economic efficiency. This definition describes the components of an adaptive material system, but does not state a goal or objective of the system. The other definition is based upon a *science paradigm*, and attempts to capture the essence of biologically inspired materials by addressing the goal as creating material systems with intelligence and life

features integrated in the microstructure of the material system to reduce mass and energy and produce adaptive functionality.

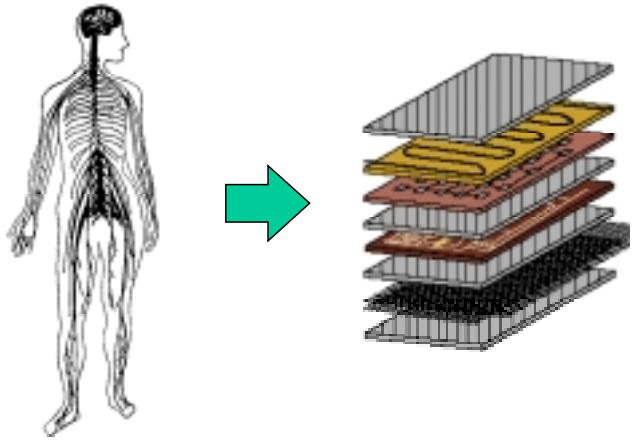

Figure 1 Biomimesis parallelism between the human body and a smart material system.

It is important to note that the science paradigm does not define the type of materials to be utilized. It does not even state definitively that there are sensors, actuators, and controls, but instead describes a philosophy of design. Biological systems are the result of a continuous process of optimization taking place over millennia. Their basic characteristics of efficiency, functionality, precision, self-repair, and durability continue to fascinate scientists and engineers alike. Smart structures have evolved by biomimesis; they aim at creating man-made structures with embedded sensing, actuation, and control capabilities. Figure 1 shows how the modern engineer might try to duplicate nature's functionalities with man-made material systems: composite materials to replicate the biological skeleton; piezo and optical sensors to duplicate the five senses; piezo and shape memory alloy actuators to replicate the fast twitch and slow twitch muscles; artificial intelligence networks to mimic the motor control system, etc. Such innovative developments have been spurred by the

revolutionary emergence of commercially available smart active materials and their sensing and actuation derivatives.

1.2 ACTIVE MATERIALS ACTUATORS

The term 'smart materials' incorporates a large variety of revolutionary material systems that exhibit sensing and actuation properties similar to that of the living world. Of these, some smart materials may have only sensing properties, other may exhibit both sensing and actuation. An example of the former are the optical fiber sensors, and composite materials incorporating such fibers in their fibrous structure. Of the latter, a most obvious example is that of piezoelectric ceramics that can both sense and create mechanical strain. We will not cover the smart sensing materials here, but rather point the reader towards the extensive bibliography on the subject (e.g., Udd, 1995). Concentrating our attention on actuating smart materials, we notice that their list is long and varied. A raw categorization may distinguish several large classes:

1. Piezoelectric (PZT), electrostrictive (PMN), and magnetostrictive (Terfenol-D) materials that directly convert an externally applied electric or magnetic field into induced strain through a direct physical effect at microstructural level (similar to the thermal expansion effect). Such materials come as piezo and electrostrictive ceramics, piezoelectric polymers, and magnetostrictive alloys.

2. Shape memory alloys (SMA) that produce induce-strain actuation through a metallurgical phase transformation triggered by the crossing of certain temperature thresholds (Martensitic to Austenitic transformation). The induced-strain effect of SMA materials is the result of the strain states not being carried over from one metallurgical phase into the other phase. Thus, a material deformed (say, stretched) in the Martensitic phase will return to the undeformed

state when transformed into the Austenitic phase, with the overall result being a net change in shape (i.e., length).

3. Electrochemical actuators, which are base on the change of volume that takes place during electrically-controlled chemical reactions.

4. Chemomechanical actuators, which start with biological muscle and continue with several 'artificial muscle' materials based on net-linked collages, polyelectrolyte gels, conducting polymers, etc. One example is provided by the electroactive polymers Nafion® and Flemion® that display remarkable large strains when used as wet membranes (Bar-Cohen and Leary, 2000).

Also mentioned by some authors (e.g., Janocha, 1999) are certain smart materials that change their effective damping properties in response to electric and magnetic stimuli:

1. Electrorheological fluids (ERF), which are suspensions of micron-size high-dielectric-strength particles in an insulating base oil, able to modify their effective viscosity and shear strength in response to electric fields.

2. Magnetorheological fluids (MRF), which are suspension of micro-size ferromagnetic particles able to modify their effective viscosity and shear strength in response to magnetic fields.

In the present discussion, we will focus our attention on the piezoelectric, electrostrictive, magnetostrictive, and shape memory alloy materials, and explain how they can be used in the construction of active-materials actuators.

Actuators are devices that produce mechanical action. They convert input energy (electric, hydraulic, pneumatic, thermic, etc.) to mechanical output (force and displacement). Actuators rely

on a “prime mover” (e.g., the displacement of high-pressure fluid in a hydraulic cylinder, or the electromagnetic force in an electric motor) and on mechanisms to convert the prime mover effect into the desired action. If the prime mover can impart a large stroke, direct actuation can be effected (e.g., a hydraulic ram). When the prime mover has small stroke, but high frequency bandwidth, a switching principle is employed to produce continuous motion through the addition of switched incremental steps (e.g., some electric motors). Like everywhere in engineering, the quest for simpler, more reliable, more powerful, easier to maintain, and cheaper actuators is continuously on. In this respect, the use of active-materials solid-state induced-strain actuators has recently seen a significant increase. Initially developed for high-frequency, low-displacement acoustic applications, these revolutionary actuators are currently expanding their field of application into many other areas of mechanical and aerospace design. Compact and reliable, induced-strain actuators directly transform input electrical energy into output mechanical energy. One application area in which solid-state induced-strain devices have a very promising future is that of linear actuation for vibration and aeroelastic control. At present, the linear actuation market is dominated by hydraulic and pneumatic pressure cylinders, and by electromagnetic solenoids and shakers.

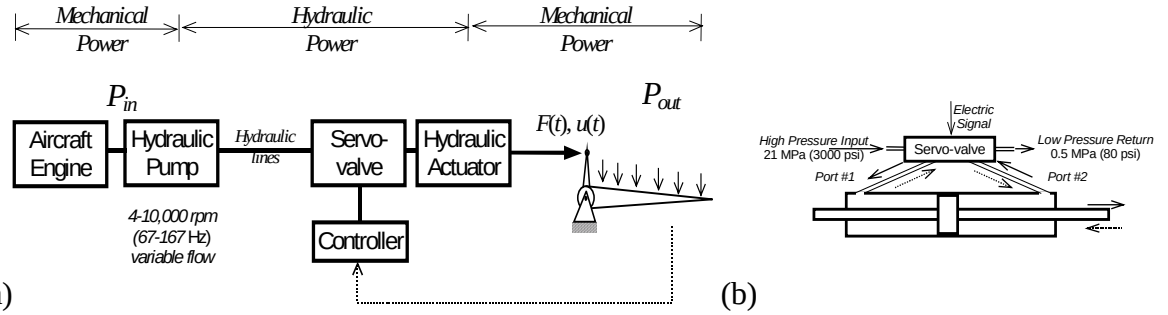

Figure 2 Conventional hydraulic actuation system: (a) flight controls of modern aircraft: (b) details of the servo-valve controlled hydraulic cylinder

Hydraulic and pneumatic cylinders offer reliable performance, with high force and large displacement capabilities. When equipped with servovalves, hydraulic cylinders can deliver variable

stroke output. Servovalve-controlled hydraulic devices are the actuator of choice for most aerospace (Figure 2), automotive, and robotic applications. However, a major drawback in the use of conventional hydraulic actuators is the need for a separate hydraulic power unit equipped with large electric motors and hydraulic pumps that send the high-pressure hydraulic fluid to the actuators through hydraulic lines. These features can be a major drawback in certain applications. For example, a 300-passanger airplane has over a kilometer of hydraulic lines spanning its body, from the engines to the most remote wing tip. Such a network a vulnerable hydraulic piping can present a major safety liability, under both civilian and military operation. In ground transportation, similar considerations have spurred automobile designers to promote the “brake-by-wire’ concept that is scheduled to enter the commercial market in the next few years. In some other applications, the use of conventional actuation is simply not an option. For example, the actuation of an aerodynamic servo-tab at the tip of a rotating blade, such as in helicopter applications, cannot be achieved through conventional hydraulic or electric methods due to the prohibitive high-g centrifugal force field environment generated during the blade rotation.

At present, electro-mechanical actuation that directly converts electrical energy into mechanical energy is increasingly preferred in several industrial applications. The most widely used high-power electro-mechanical actuators are the electric motors. However, they can deliver only rotary motion and need to utilize gearboxes and rotary-to-linear conversion mechanisms to achieve linear motion. This route is cumbersome, leads to additional weight, and has low frequency bandwidth. Direct conversion of electrical energy into linear force and motion is possible, but its practical implementation in the form of solenoids and electrodynamic shakers is marred by typically low-force performance. The use of solenoids or electrodynamic shakers to perform the actuator duty-cycle of hydraulic cylinders does not seem conceivable.

Solid-state induced-strain actuators offer a viable alternative (Figure 3). Though their output displacement is relatively small, they can produce remarkably high force. With well-architectured displacement amplification, induced-strain actuators can achieve output strokes similar to those of conventional hydraulic actuators, but over much wider bandwidth. Additionally, unlike conventional hydraulic actuators, solid-state induced-strain actuators do not require separate hydraulic power units and long hydraulic lines, and use the much more efficient route of direct electric supply to the actuator site.

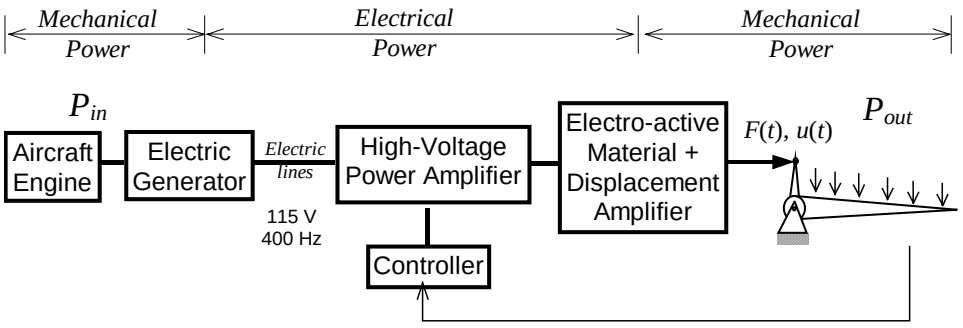

Figure 3 Schematic representation of a solid-state induced-strain actuated flight control system using electro-active materials.

The development of solid-state induced-strain actuators has entered the production stage, and actual actuation devices based on these concepts are likely to reach the applications market in the next few years. An increasing number of vendors are producing and marketing solid-state actuation devices based on induced-strain principles.

2 PIEZOELECTRIC AND ELECTROSTRICTIVE MATERIALS

2.1 PIEZOELECTRICITY

Piezoelectricity (discovered in 1880 by Jacques and Pierre Curie) describes the phenomenon of generating an electric field when the material is subjected to a mechanical stress (direct effect), or,

conversely, generating a mechanical strain in response to an applied electric field. Piezoelectric properties occur naturally in some crystalline materials, e.g., quartz crystals (SiO_2), and Rochelle salt. The latter is a natural ferroelectric material, possessing an orientable domain structure that aligns under an external electric field and thus enhances its piezoelectric response. Piezoelectric response can also be induced by electrical poling certain polycrystalline materials, such as piezoceramics (Figure 4).

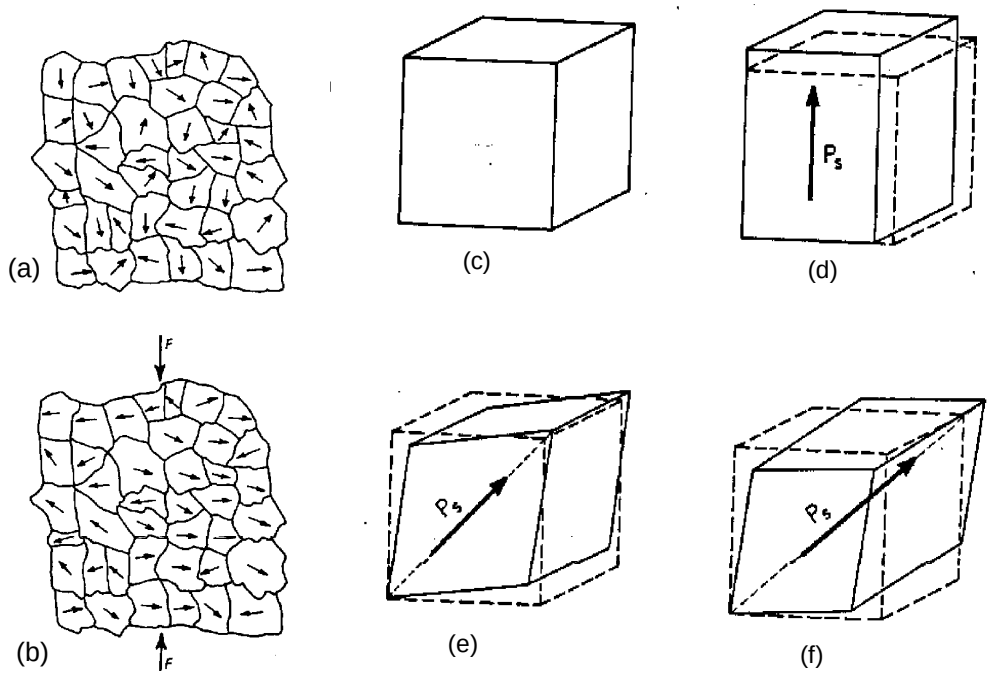

Figure 4 Illustration of piezoelectric principles: (a) un-stressed piezoelectric material has the electric domains randomly oriented; (b) stressing produces orientation of the electric domains perpendicular to the loading direction; (c) Cubic phase, stable above the Curie temperature, no piezoelectricity; (d) Tetragonal phase; (e) Orthorhombic phase; (f) Rhombohedral phase (after Clark, 1986)

The application of a high poling field at elevated temperatures results in the alignment of the crystalline domains; this alignment is locked in place when the high temperatures are removed. Subsequently, the poled ceramics response to the application of an applied electric field or mechanical stress with typical piezoelectric behavior. The distortion of the crystal domains produces the piezoelectric effect. Lead Zirconate Titanate, $PbZrO_3$, commercial known as PZT. To date, many

PZT formulations exist, the main differentiation being between "soft" (e.g., PZT 5-H) and "hard" (e.g., PZT 8). Within the linear range, piezoelectric materials produce strains that are proportional to the applied electric field or voltage. Induced strains in excess of 1000 μstrain (0.1%) have become common. These features make piezoelectric materials very attractive for a variety of sensor and actuator applications.

2.2 MODELING OF PIEZOELECTRIC BEHAVIOR

For linear piezoelectric materials, the interaction between the electrical and mechanical variables can be described by linear relations (ANSI/IEEE Standard 176-1987). A tensorial relation between mechanical and electrical variables is established in the form:

$$\begin{aligned} S_{ij} &= s^{E}_{ijkl} T_{kl} + d_{kij} E_k + \alpha^{E}_{i} \theta \\ D_j &= d_{jkl} T_{kl} + \varepsilon^{T}_{jk} E_k + \tilde{D}_m \theta \end{aligned} \tag{1}$$

where S_{ij} is the mechanical strain, T_{ij} is the mechanical stress, E_i is the electrical field, D_i is the electrical displacement (charge per unit area), s^{E}_{ijkl} is the mechanical compliance of the material measured at zero electric field (E = 0), ε^{T}_{jk} is the dielectric constant measured at zero mechanical stress (T = 0); d_{kij} is the piezoelectric displacement coefficient that couples the electrical and mechanical variables, θ is the absolute temperature, α^{E}_{i} is the coefficient of thermal expansion under constant electric field; $\tilde{D}_j$ is the electric displacement temperature coefficient. The stress and strain are second order tensors, while the electric field and the electric displacement are first order tensors. The superscripts *T, D; E* signify that the quantities are measured at zero stress, or zero current, or constant electric field, respectively. The second equation reflects the *direct piezoelectric effect*, while the first equation refers to the *converse piezoelectric effect*.

In engineering practice, the tensorial Equation (1) is rearranged in matrix form using the 6-components stress and strain vectors, (T_1 … T_6) and (S_1 … S_6), where the first 3 components represent direct stress and strain, while the last three represent shear. Figure 5 illustrates the physical meaning of these equations in the case of simple polarization. Figure 5a shows that an electric field $E_3 = V/t$ applied parallel to the direction of polarization ($E_3 \parallel P$) induces thickness expansion ($\varepsilon_3 = d_{33}E_3$) and transverse retraction ($\varepsilon_1 = d_{31}E_3$). Figure 5b shows that, if the field is perpendicular to the direction of polarization ($E_3 \perp P$), shear deformation is induced ($\varepsilon_5 = d_{15}E_3$).

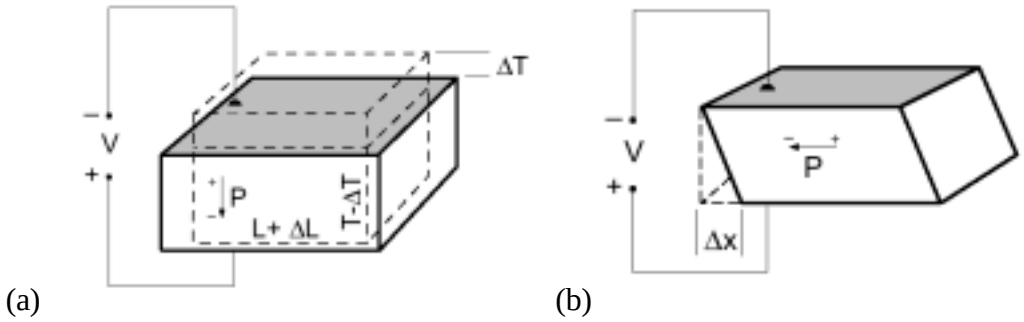

(a) (b)

Figure 5 Basic induce-strain responses of piezoelectric materials: (a) axial and transverse strain; (b) shear strain (after Piezo Systems, Inc.)

Electromechanical coupling coefficient is defined as the square root of the ratio between the mechanical energy stored and the electrical energy applied to a piezoelectric material. For direct-actuation, we have $\kappa_{33} = d_{33}/\sqrt{s_{11}\varepsilon_{33}}$, while for transverse actuation, $\kappa_{31} = d_{31}/\sqrt{s_{11}\varepsilon_{33}}$.

2.3 ELECTROSTRICTIVE MATERIALS

Electrostrictive ceramics are ferroelectric ceramics that contain both linear and quadratic terms:

$$\begin{aligned} S_{ij} &= s^E_{ijkl}T_{kl} + d_{kij}E_k + M_{klij}E_kE_l \\ D_j &= d_{jkl}T_{kl} + \varepsilon^T_{jk}E_k \end{aligned} \quad . \tag{2}$$

Note that the first two terms in the first equation are the same as for piezoelectric materials. The third term is due to electrostriction, with M_{klij} being the electrostrictive coefficient. In general, the piezoelectric effect is possible only in noncentrosymmetric materials, whereas the electrostrictive effect is not limited by symmetry and is present in all materials. A common electrostrictive compound is Lead-Magnesium-Niobate, or PMN. Commercially available PMN formulations are internally biased and optimized to give quasi-linear behavior, but do not accept field reversal. Figure 6 compares induced-strain response of some commercially available piezoelectric, electrostrictive, and magnetostrictive actuation materials. It can be seen that the electrostrictive materials have much less hysteresis, but more non-linearity.

2.4 PIEZOPOLYMERS

Polyvinylidene fluoride, abbreviated PVDF or PVF_2, is a polymer with strong piezoelectric and pyroelectric properties. In the α phase, PVDF is not polarized and is used as a common electrical insulator among many other applications. To impart the piezoelectric properties, the α phase is converted to the β phase and polarized. Stretching α-phase material produces the β phase. After surface metallization; a strong electric field is applied to provide permanent polarization. The flexibility of the PVDF overcomes some of the drawbacks associated with the piezoelectric ceramics brittleness. As a sensor, PVDF provides higher voltage/electric field in response to mechanical stress. Their piezoelectric g-constants (i.e., the voltage generated per unit mechanical stress) are typically 10 to 20 times larger than for piezoceramics. PVDF film also produces an electric voltage in response to infrared light due to its strong pyroelectric coefficient. However, the use of PVDF materials as actuators is inappropriate for most structural applications due to their low elastic modulus which cannot generate large actuation forces.

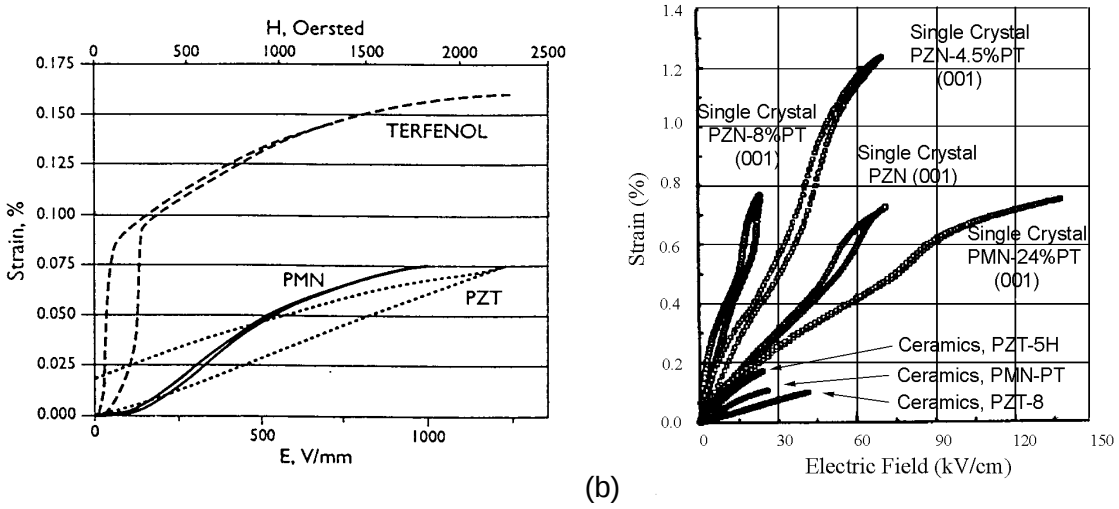

Figure 6 Strain vs. electric field behavior of induced strain materials: (a) currently available materials (Giurgiutiu *et al.,* 1995); (b) new <001> oriented rhombohedral crystals of PZN-PT and PMN-PT compared to current piezoelectric ceramics (Park and Shrout, 1997).

2.5 NEW PIEZOELECTRIC MATERIALS

New piezoelectric materials with much larger induced-strain capabilities are currently being developed in research laboratories. Very promising are the single crystal materials. Park and Shrout (1997) studied single crystals of PZN-PT, a relaxor pervoskite $Pb(Zn_{1/3}Nb_{2/3})O_3 - PbTiO_3$. Strain levels of up to 1.5%, and reduced hysteresis have been reported. The response of these new materials can be an order of magnitude larger than that of conventional PZT materials (see curves in Figure 6b). When building actuators from PZN-PT material, one must take into account the strong dependence of the piezoelectric properties on the crystal orientation. This imposes certain design restrictions in comparison with conventional piezoceramics. Commercial production of induced strain actuators based on these new materials has been undertaken by TRS Ceramics, Inc., and a prototype PZN-PT actuator with a maximum strain of around 0.3% has been reported.

Table 1 Mechanic and dielectric properties for piezoelectric (PZT-5, PZT-8) and electrostrictive (PMN EC-98) materials

Property	Soft PZT-5 Navy Type VI	Hard PZT-8 Navy Type III	PMN EC-98
ρ (kg/m^3)	7600	7600	7850
k_{31}	0.36	0.31	0.35
k_{33}	0.71	0.61	0.72
k_{15}	0.67	0.54	0.67
d_{31} (x10^{-12}m/V)	-270	-100	-312
d_{33} (x10^{-12}m/V)	550	220	730
d_{15} (x10^{-12}m/V)	720	320	825
g_{31} (x10^{-3}Vm/N)	-9.0	-11.3	-6.4
g_{33} (x10^{-3}Vm/N)	18.3	24.9	15.6
g_{15} (x10^{-3}Vm/N)	23.9	36.2	17
s_{11}^E (x10^{-12} m^2/N)	15.9	10.6	16.3
Poisson ratio	0.31	0.31	0.34
s_{33}^E (x10^{-12} m^2/N)	20.2	13.2	21.1
Curie Temp. (^{0}C)	200	350	170
Mechanical Q_M	75	900	70

2.6 ADVANTAGES AND LIMITATIONS OF PIEZOELECTRIC AND ELECTROSTRICTIVE ACTUATION MATERIALS

Piezoelectric ceramics, e.g., PZT, are essentially small-stroke large-force solid-state actuators with very good high-frequency performance. However, they also display certain limitations. The most obvious limitation is that, in many engineering applications, some form of mechanical amplification is required. Other limitations are associated with electrical breakdown, depoling, Curie temperature, non-linearity, and hysteresis.

Electrical Breakdown may happen when an electric field applied in the poling direction exceed the dielectric strength of the material, resulting in electrical arcing through the material and short-circuit. Electrical breakdown also destroys the piezoelectric properties of the material.

Depoling may happens when an electric field is applied opposite to the poling direction, resulting in degradation of the piezoelectric properties or even polarization in the opposite direction. The depoling field (*a.k.a.* coercive field) may be as low as half of the electrical breakdown field.

Curie Temperature. At temperatures close to the Curie temperature, depoling is facilitated, aging and creep are accelerated, and the maximum safe mechanical stress is decreases. For typical PZT materials, the Curie temperature is about 350°C. The operating temperature should generally be at least 50^0C lower than the Curie temperature.

Non-linearity and Hysteresis. Real-life piezoceramics are non-linear and hysteretic (Figure 6). Hysteresis is due to internal sliding events in the polycrystalline piezoelectric material. Upon removal of the electric field, remnant mechanical strain is observed. Hysteresis of common piezoelectric may range from 1 to 10%. Under high frequency operation, hysteresis may generate excessive heat, and loss of performance may occur if the Curie temperature is exceeded.

The main advantage of electrostrictive materials over piezoelectric materials is their very low hysteresis. This could be especially beneficial in high-frequency dynamic applications, which could involve considerable hysteresis-associated heat dissipation. The main disadvantage of electrostrictive materials is the temperature dependence of their properties.

3 MAGNETOSTRICTIVE MATERIALS

Magnetostrictive materials expand in the presence of a magnetic field, as their magnetic domains align with the field lines. Magnetostriction was initially observed in nickel cobalt, iron, and their alloys but the values were small (<50 μstrain). Large strains (~10,000 μstrain) were observed in the rare-earth elements terbium (Tb) and dysprosium (Dy) at cryogenic temperatures (below 180^0K). The compound Terfenol-D ($Tb_{.3}Dy_{.7}Fe_{1.9}$), developed at Ames Laboratory and the Naval Ordnance

Laboratory (now Naval Surface Weapons Center), displays magnetostriction of up to 2000 μstrain at room temperature and up to 80° C and higher (Clark, 1980, 1986, 1992; Lachisserie, 1993).

3.1 MODELING OF THE MAGNETOSTRICTIVE MATERIALS

The magnetostrictive constitutive equations contain both linear and quadratic terms:

$$\begin{aligned} S_{ij} &= s^{E}_{ijkl} T_{kl} + d_{kij} H_k + M_{klij} H_k H_l \\ B_j &= d_{jkl} T_{kl} + \mu^{T}_{jk} H_k \end{aligned} \tag{3}$$

where, in addition to the already defined variables, H_k is the magnetic field intensity, B_j is the magnetic flux density, and μ^{T}_{jk} is the magnetic permeability under constant stress. The coefficients d_{kij} and M_{klij} are defined in terms of magnetic units. The magnetic field intensity, *H*, in a rod surrounded by a coil with n turns per unit length is related to the current, *I*, through the relation:

$$H = nI \tag{4}$$

3.2 ADVANTAGES AND LIMITATIONS OF MAGNETOSTRICTIVE ACTUATORS

Magnetostrictive materials, like Terfenol-D, are essentially small-stroke large-force solid-state actuators that have wide frequency bandwidth. However, they also display certain limitations. The most obvious one is that, in actuation applications, some form of mechanical amplification is required. The main advantage of magnetoactive actuation materials over electroactive materials may be found in the fact that it is sometimes easier to create a high intensity magnetic field than a high intensity electric field. High electric fields require high voltages, which raise important insulation and electric safety issues. According to Equation (4), high magnetic fields could be realized with lower voltages using coils with a large number of turns per unit length, through which a high-amperage current flows.

An important limitation of the magnetoactive materials is that they cannot be easily energized in the2-D topology, as when applied to a structural surface. This limitation stems from the difficulty of creating high-density magnetic fields without a closed magnetic circuit armature. For the same reason, the magnetoactive induced-strain actuators will always require additional construction elements besides the magnetoactive materials. While a bare-bones electroactive actuator need not contain anything more than just the active material, the bare-bones magnetoactive actuator always needs the energizing coil and the magnetic circuit armature. For this fundamental reason, the power density (either per unit volume or per unit mass) of magnetoactive induced-strain actuators will always remain below that of their electroactive counterparts.

4 SHAPE MEMORY ALLOYS

Another class of induced strain actuating materials, with much larger strain response but low frequency bandwidth, is represented by shape memory alloys. Shape memory alloys (SMA) materials are thermally activated ISA materials that undergo phase transformation when the temperature passes certain values. The metallurgical phases involved in this process are the low-temperature Martensite and the high-temperature Austenite. When phase transformation takes place, the SMA material modifies its shape, i.e., it has ‘memory’. The SMA process starts with the material being annealed at high-temperature in the Austenitic phase (Figure 7). In this way, a certain shape is ‘locked’ into the material. Upon cooling the material transforms into the Martensitic phase, and adopts a twinned crystallographic structure. When mechanical deformation is applied, the twinned crystallographic structure switches to a skew crystallographic structure. Strains as high a 8% can be achieve through this de-twinning process. This process give the appearance of permanent plastic deformation, though no actual plastic flow took place. In typical actuator applications, this process is used to store mechanical energy by stretching SMA wires.

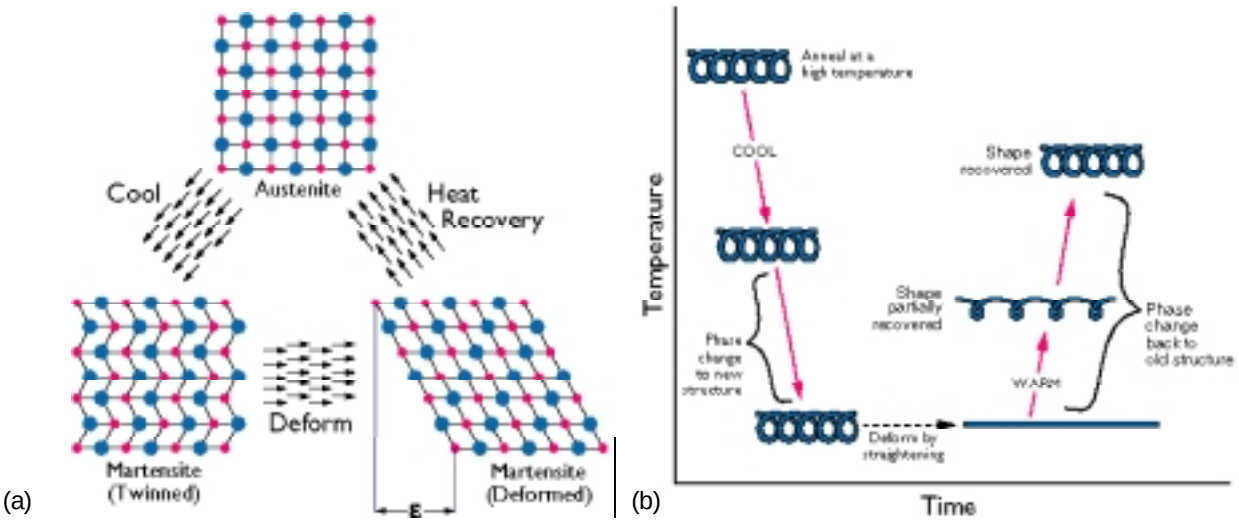

Figure 7 Principles of SMA materials: (a) change in crystallographic structure during cooling and heating (after Duering *et al.*, 1990, page 11); (b) associated component-shape changes, using a coil spring as an example (after Udd, 1995, page 515).

Upon heating, the Martensitic phase changes into Austenite and the shape initially imposed by annealing is recovered. In this way, the permanent deformation created through de-twinning of the Martensitic phase is removed, and the material returns to its initial state memorized during annealing at Austenite temperatures. If recovery is mechanically prevented, restraining stresses of up to 700 MPa can be developed. This is the one-way shape memory effect, which is a one-time only deployment at the end of which full recovery of the initial state is obtained. For dynamic operations, a two-way shape memory effect is preferred, in order that cyclic loading and unloading is attained. Two-way shape memory effect can be achieved through special thermomechanical 'training' of the material. In such cases, repeated activation of SMA strains is possible in synch with heating-cooling cycles

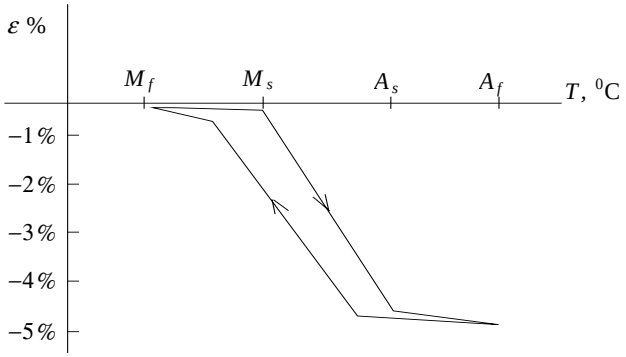

Figure 8 Schematic representation of strain recovery through the SMA effect in a two-way shape memory alloy (after Lagoudas, 1995).

(Figure 8). Many materials are known to exhibit the shape-memory effect (Bank, 1975). They include the copper alloy systems of Cu-Zn, Cu-Zn-Al, Cu-Zn-Ga, Cu-Zn-Sn, Cu-Zn-Si, Cu-Al-Ni, Cu-Au-Zn; Cu-Sn, the alloys of Au-Cd, Ni-Al; Fe-Pt; others. The most common shape-memory alloy is the Nickel-Titanium compound, Nitinol™, discovered in 1962 by Buehler *et al.* at the Naval Ordnance Laboratory (NOL).

During heating, the change from Martensite to Austenite starts at temperature A_s and finishes at temperature A_f. During cooling, the reverse change from Austenite to Martensite starts at temperature M_s and finishes at temperature M_f. Note that $A_s < A_f$,while $M_s > M_f$. In the interval (A_s, A_f) on heating, and (M_s, M_f) on cooling, two phases coexist in temperature-dependent volume fractions. The values of the phase-transition temperatures can be varied with alloy composition and stress level. In fact, in SMA materials, stress and temperature act in opposition such that an SMA material brought to Austenite by heating can be isothermally forced back to Martensite by stressing. Shape memory alloys composition can be tuned to start the Austenite transformation at almost any predetermined temperature in the range -50^0C to 62^0C (Barrett, 1995).

In addition to "memory", SMA materials have other remarkable properties: phase-dependent elastic modulus, superelasticity, and high internal damping. In most metals, the elastic modulus decreases with temperature: in SMA materials it actually increases, since the modulus of the high-temperature Austenitic phase can be up to 3 times larger than that of the low-temperature Martensitic phase. Superelasticity is associated with the fact that strains of up to 12% can be accommodated before actual plastic deformation starts to take place. Superelasticity is displayed by low-A_f SMA materials, which are Austenitic at room temperature. As stress is applied, the superelastic SMA material undergoes phase transformation and goes into Martensite. Upon unloading, the Austenite phase is recovered, and the material returns to the zero-stress zero-strain state, i.e., displays

superelastic properties (Figure 9). Though full strain recovery has been achieved, the recovery is nonlinear and follows a hysteretic path. The internal damping of the SMA materials is associated with the hysteresis curve enclosed by the loading-unloading cycle. The area within this cycle is orders of magnitude larger than for conventional elastic materials.

4.1 MODELING OF SMA MATERIALS

Since the mechanical behavior of SMA materials is closely related to the microscopic martensitic phase transformation, the constitutive relations developed for conventional materials such as Hooke's law and plastic flow theory are not directly applicable. Hence, specific constitutive relations, which take into consideration the phase transformation behavior of SMA, have been developed (Cory, 1978; Muller, 1979; Tanaka and Nagaki, 1982). Two approaches are generally used: (a) the phenomenological (macroscopic) approach, based on extensive experimental work; and (b) the physical (microscopic) approach using fundamental physical concepts. Hybrid approaches that combine both approaches to obtain a more accurate description and prediction of the SMA material behavior have also been used. Tanaka's model, based on the concept of the free-energy driving force, considers a one-dimensional metallic material undergoing phase transformation. The state variables for the material are strain, ε, temperature, T, and Martensitic fraction, ξ. Then, a general state variable, Λ, is defined as

$$\Lambda = (\bar{\varepsilon}, T, \xi) \tag{5}$$

The Helmholtz free energy is a function of the state variable Λ. The general constitutive relations are then derived from the first and second laws of thermodynamics as

$$\bar{\sigma} = \rho_0 \frac{\partial \Phi}{\partial \bar{\varepsilon}} = \sigma(\bar{\varepsilon}, T, \xi) \tag{6}$$

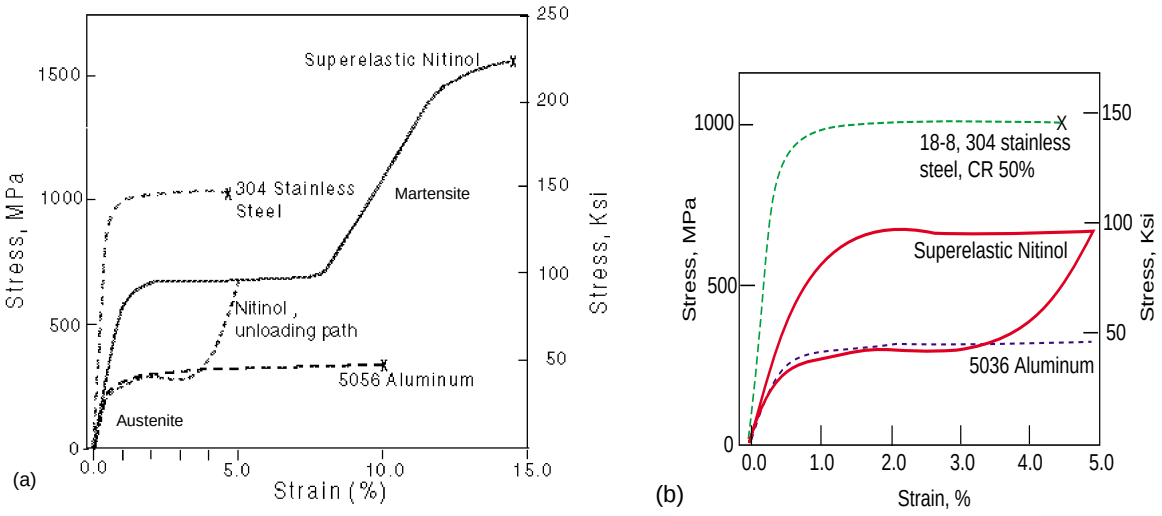

Figure 9 Stress-strain curves of superelastic Nitinol and other metallic wires: (a) overall behavior (Paine and Rogers, 1994); (b) zoom-in on the low-strain range (Paine and Rogers, 1995).

The stress is a function of the Martensite fraction, an internal variable. Differentiation of Equation (6) yields the stress rate equation:

$$\dot{\sigma} = \frac{\partial \sigma}{\partial \varepsilon}\dot{\varepsilon} + \frac{\partial \sigma}{\partial T}\dot{T} + \frac{\partial \sigma}{\partial \xi}\dot{\xi} = D\dot{\varepsilon} + \Theta\dot{T} + \Omega\dot{\xi} \tag{7}$$

where D is Young's modulus, Θ is the thermoelastic tensor, and Ω is the transformation tensor, a metallurgical quantity that represents the change of strain during phase transformation. The Martensite fraction, ξ, can be assumed as an exponential function of stress and temperature:

$$\xi_{M\to A} = \exp\left[A_a(T - A_s) + B_a\sigma\right],\ \xi_{A\to M} = 1 - \exp\left[A_m(T - M_s) + B_m\sigma\right] \tag{8}$$

where A_a, A_m, B_a; B_m are material constants in terms of the transition temperatures, A_s, A_f, M_s; M_f.

Liang and Rogers (1990) derived a constitutive equation by the time-integration of Equation (7)

$$\sigma - \sigma_0 = D(\varepsilon - \varepsilon_0) + \theta(T - T_0) + \Omega(\xi - \xi_0). \tag{9}$$

For this, a cosine model for the phase transformation was adopted, i.e.,

$$\xi_{A\to M} = \frac{\xi_M}{2}\left\{\cos\left[a_A(T-A_s)+b_A\sigma\right]+1\right\},\ \xi_{M\leftarrow A} = \frac{1-\xi_A}{2}\left\{\cos\left[a_M(T-M_s)+b_{M\sigma}\right]+1\right\}+\frac{1+\xi_A}{2} \qquad (10)$$

where $a_A = \dfrac{\pi}{A_f - A_s}$, $a_M = \dfrac{\pi}{M_s - M_f}$, $b_A = -\dfrac{a_A}{C_A}$, $b_M = -\dfrac{a_M}{C_M}$ while C_M and C_A are slopes.

4.2 ADVANTAGES AND LIMITATIONS OF SMA ACTUATION

The main advantage of SMA materials is their capability to produce sizable (up to 8%) actuation strains. In addition, they have inherent simplicity since only heating (readily available through the electric Joule effect) is needed for actuation. Main limitations of the SMA actuators are the poor energy conversion efficiency, and the low bandwidth of the heating/cooling process which can only achieve a few Hz, at the very best.

5 EFFECTIVE IMPLEMENTATION OF INDUCED-STRAIN ACTUATION

5.1 DESIGN AND CONSTRUCTION OF PIEZOELECTRIC AND ELECTROSTRICTIVE ACTUATORS

An electroactive solid-state actuator consists of a stack of many layers of electroactive material (PZT or PMN) alternatively connected to the positive and negative terminals of a high voltage source (Figure 10a). Such a PZT or PMN stack behaves like an electrical capacitor. When activated, the electroactive material expands and produces output displacement. The PZT or PMN stacks are constructed by two methods. In the first method, the layers of active material and the electrodes are mechanically assembled and glued together using a structural adhesive. The adhesive modulus (typically, 4-5 GPa) is at least an order of magnitude lower than the modulus of the ceramic (typically, 70-90 GPa). This aspect may lead to the stack stiffness being significantly lower than the stiffness of the basic ceramic material. In the second method, the ceramic layers and the electrodes are assembled in the "green" state. Then, they are fired together (co-fired) under a high isostatic

pressure (HIP process) in the processing oven. This process ensures a much stiffer final product and, hence, a better actuator performance. However, the processing limitations, such as oven and press size, etc., do not allow the application of this process to anything else but small-size stacks.

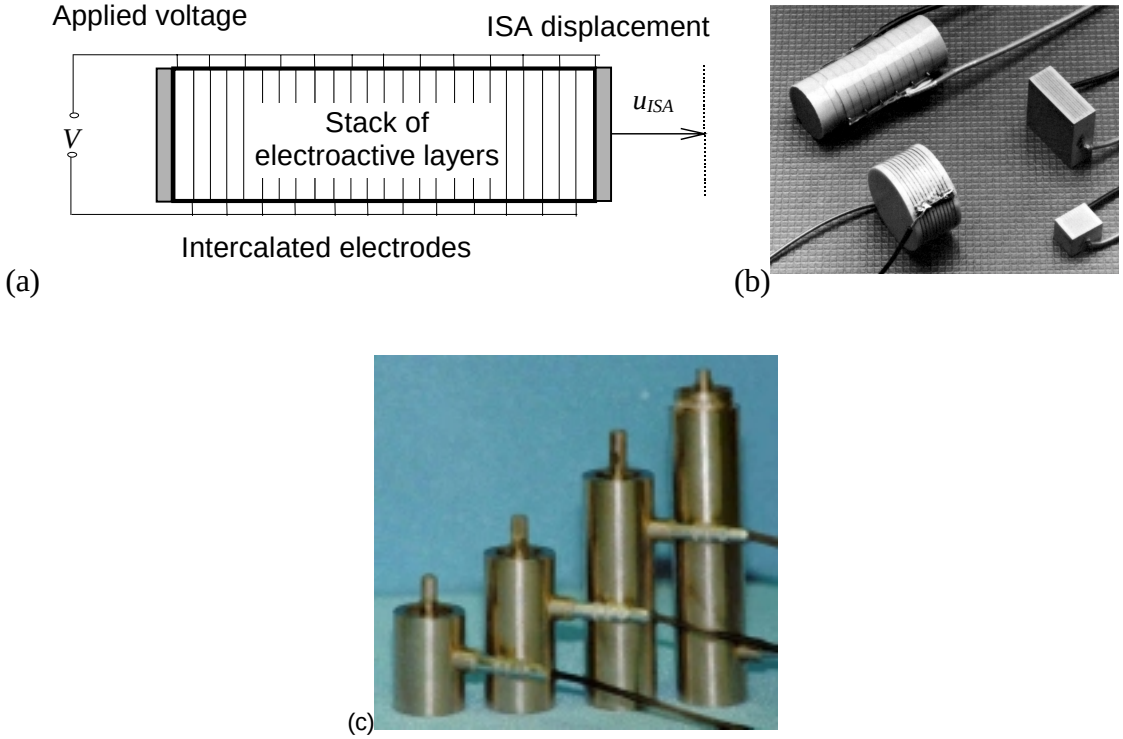

Figure 10 Induced strain actuator using a PZT or PMN electroactive stack: (a) schematic; (b) typical commercially available cofired stack from EDO Corporation; (c) a range of Politech PI actuators heavy-duty actuators.

The PZT and PMN stacks may be surrounded by a protective polymeric or elastomeric wrapping. Lead wires protrude from the wrapping for electrical connection. Steel washers, one at each end, are also provided for distributing the load into the brittle ceramic material. When mounted in the application structure, these stacks must be handled with specialized knowledge. Protection from accidental impact damage must be provided. Adequate structural support and alignment are needed. Mechanical connection to the application structure must be such that neither tension stresses nor bending are induced in the stack since the active ceramic material has low tension strength. Hence, the load applied to the stack must always be compressive and perfectly centered. If tension loading

is also expected, adequate pre-stressing must be provided through springs or other means. For applications, the stack can be purchased as such (Figure 10b), or encapsulated into a steel casing which provides a prestress mechanism and the electrical and mechanical connections (Figure 10c).

Figure 11 compares the response of two commercially available actuators, one piezoelectric, the other electrostrictive. It can be seen that both have about the same maximum induced-strain value, as it can be readily verified by dividing the maximum displacement by the actuator length. Both material types display quasi-linear behavior. The piezoelectric actuator allows some field reversal (up to 25%, according to manufacturer), which make the total stroke larger. On the other hand, the electrostrictive actuator has much less hysteresis, i.e., less losses and less heating in high-frequency regime.

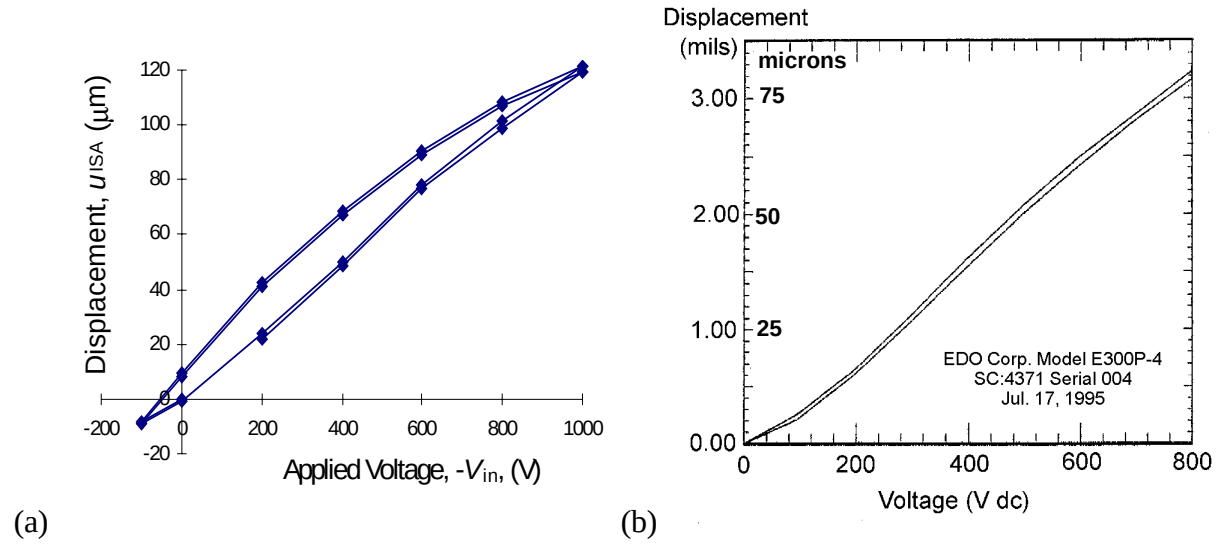

Figure 11 The induced-strain displacement *vs.* applied voltage for typical electroactive actuators: (a) PI P-245.70 PZT stack, 99-mm long (Giurgiutiu *et al.*, 1997b); (b) EDO Corporation model E300P PMN stack, 57 mm long.

5.2 DESIGN AND CONSTRUCTION OF MAGNETOSTRICTIVE ACTUATORS

Magnetostrictive materials can be also used to produce an effective actuator. Figure 12a shows the typical layout of a magnetostrictive actuator. It consists of a Terfenol-D bar surrounded by an electric coil and enclosed into an annular magnetic armature. The magnetic circuit is closed through end caps . In this arrangement, the magnetic field is strongest in the cylindrical inner region filled by the Terfenol-D bar. When the coil is activated, the Terfenol-D expands and produces output displacement. The Terfenol-D bar, the coil, and the magnetic armature are assembled with prestress between two steel-washers and put inside a protective wrapping to form the basic magnetoactive induced-strain actuator. Thought the Terfenol-D material has been shown to be capable of up to 2000 μstrain, its behavior is highly nonlinear in both magnetic field response and the effect of compressive prestress. Manufacturers of magnetostrictive actuators optimize the internal prestress and magnetic bias to get a quasi-linear behavior in the range of 750-1000 μm/m. Figure 12b shows the displacement-magnetic field response for a typical large-power magnetostrictive actuator (ETREMA AA-140J025, 200 mm long, ≈1 kg weight, 0.140 mm peak-to-peak output displacement).

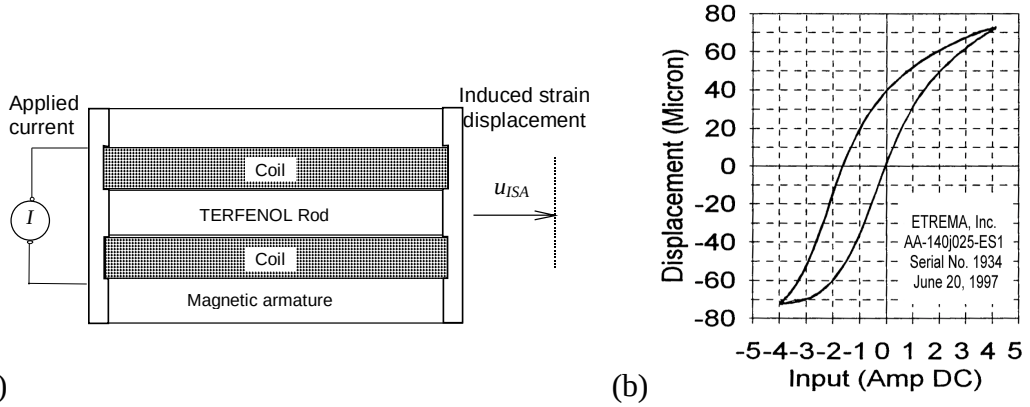

Figure 12: (a) Schematic construction of a magnetostrictive (Terfenol-D) solid-state actuator; (b) typical response curve (actuator model # AA140J025-ES1, ETREMA, Inc.)

5.3 PRINCIPLES OF INDUCED-STRAIN STRUCTURAL ACTUATION

In structural applications, the induce-strain actuators must work in direct relation with the actuated structure, and special attention must be given to their interaction. The main differentiating feature between active materials actuators and conventional actuators lies in the amount of available displacement. The induced-strain effect present in active materials results in output displacements that seldom exceed 100 microns (0.1 mm). In a conventional actuator, e.g., a hydraulic cylinder, displacement of the order of several millimeters can be easily be achieved, and if more displacement is needed, additional hydraulic fluid could be pumped in. In contrast, an induced-strain actuator has at its disposal only the very limited amount of displacement generated by the induced-strain effect. This limited displacement needs to be carefully managed, if the desired effect is to be achieved. Under reactive service loads, the internal compressibility of the active materials actuator 'eat-ups' part of the induced-strain displacement, and leads to reduced output displacement (Figure 13a). If the external stiffness, k_e, is reduced, the force in the actuator is also reduced, and more displacement is seen at the actuator output end. For a free actuator, i.e., under no external reaction, the output displacement is maximum. However, no active work is being done in this case since the force is zero. At the other extreme, when the actuator is fully constrained, the force is maximum, but no work is again performed since the displacement is zero. An optimum is attained between these two extremes, and this optimum can be best described in terms of *stiffness match* principle. Under static conditions, the stiffness match principle implies that the external stiffness (i.e., the stiffness of the application) and the internal stiffness of the actuator are equal, which gives a stiffness ratio with value $r = 1$. As shown in Figure 13b, $r = 1$ corresponds to maximum energy situation.

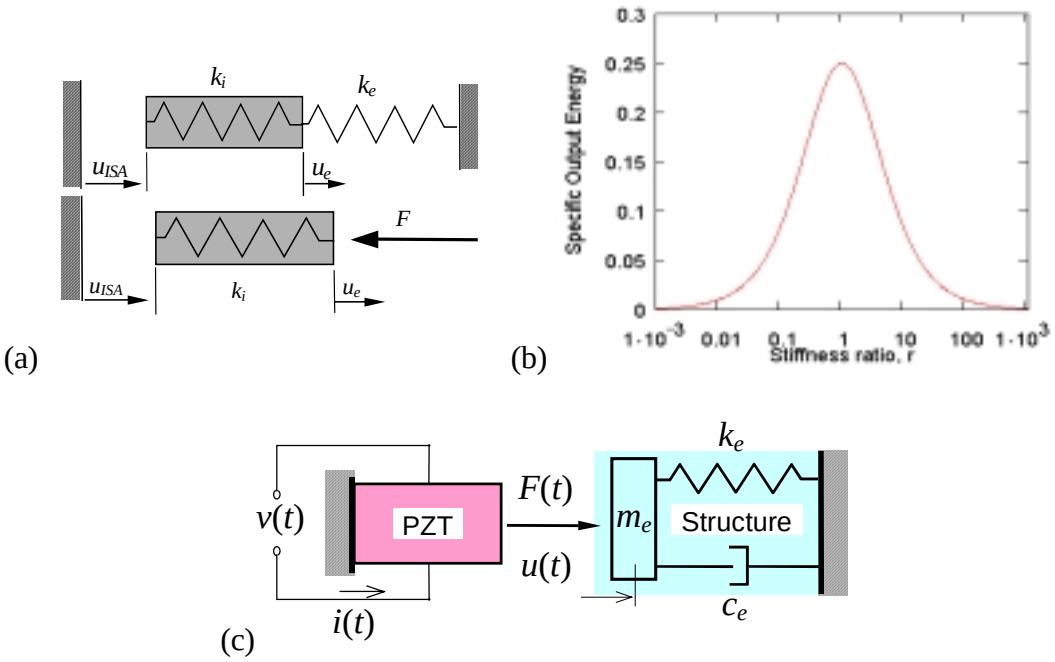

Figure 13 Schematic of the interaction between an active material actuator and an elastic structure: (a) the activate displacement, u_{ISA}, is partially lost due to the actuator internal compressibility, such that the resulting external displacement, u_e, is always less; (b) maximum energy extraction is attained when the internal and external stiffness match; (c) under dynamic conditions, the frequency dependent dynamic stiffness must be used.

Under dynamic conditions, this principle can be expressed as *dynamic stiffness match* or *impedance match.* Figure 13c shows a solid-state induced-strain actuator operating against a dynamic load with parameters $k_e(\omega)$, $m_e(\omega)$, and $c_e(\omega)$. The actuator is energized by a variable voltage, $v(t)$, which sends a time varying current, $i(t)$. The actuator output displacement and force are, $u(t)$ and $F(t)$, respectively. The complex stiffness ratio is given by

$$\bar{r}(\omega) = \bar{k}_e(\omega) / \bar{k}_i , \tag{11}$$

where $\bar{k}_e(\omega) = (k_e - \omega^2 m_e) + \mathrm{i}\omega c$ is the complex external stiffness of the dynamic load, and $\bar{k}_i$ is the complex internal stiffness of the induced strain actuator.

5.4 POWER AND ENERGY EXTRACTION FROM INDUCED STRAIN ACTUATORS

Using the definition, *mechanical power = force × velocity,* and assuming harmonic motion, we express the complex power as $\overline{P} = \frac{1}{2}\overline{F}\cdot\overline{v}^*$, where, $\overline{v}^*$ is the complex conjugate of $\overline{v}$, and $\overline{v} = i\omega\,\overline{u}$. Hence (Giurgiutiu *et al.*, 1997b), we write the output mechanical power and energy as:

$$\overline{P}_{\text{mech}} = \frac{1}{2}\overline{k}_e\overline{u}(i\omega\,\overline{u})^* = -i\omega\frac{\overline{r}(\omega)}{\left(1+\overline{r}(\omega)\right)\left(1+\overline{r}(\omega)\right)^*}\left[\frac{1}{2}\overline{k}_i\hat{u}_{ISA}^2 \right. \quad . \tag{12}$$

$$\overline{E}_{\text{mech}} = \frac{1}{2}\overline{k}_e\overline{u}(\,\overline{u})^* = \frac{\overline{r}(\omega)}{\left(1+\overline{r}(\omega)\right)\left(1+\overline{r}(\omega)\right)^*}\left[\frac{1}{2}\overline{k}_i\hat{u}_{ISA}^2 \right. \quad . \tag{13}$$

The maximum output power and energy are attained at the dynamic stiffness match condition,

$$P_{\text{out}}^{\max} = \omega\frac{1}{4}E_{\text{mech}}^*, \qquad E_{\text{out}}^{\max} = \frac{1}{4}E_{\text{mech}}^*, \tag{14}$$

where $E_{\text{mech}}^* = \frac{1}{2}k_i\hat{u}_{\text{ISA}}^2$.

5.5 ELECTRICAL INPUT POWER AND ENERGY

From the electrical side, we note that, for frequencies well below the actuator free resonance (typically, 1 to 10 kHz, depending on length), the wave propagation effects can be ignored, and the equivalent input admittance as seen at the actuator terminals is (Giurgiutiu *et al.*, 1997b):

$$Y_C(\omega) = i\omega C\left(1-\kappa_C^2\frac{\overline{r}(\omega)}{1+\overline{r}(\omega)} \right. \quad , \tag{15}$$

where, $\kappa^2 = d^2/(\overline{s}\cdot\overline{\varepsilon})$ and $\overline{s} = (1-i\delta_s)s$, $\overline{\varepsilon} = (1-i\delta_\varepsilon)\varepsilon$, δ_s is the hysteresis internal damping coefficient of the actuator, δ_ε is the dielectric loss coefficient of the actuator, $d = \frac{u_{ISA}}{V}\frac{t}{l}$, $\varepsilon = \frac{C}{A}\frac{t^2}{l}$,

$s = \frac{A}{lk_i}$, l is the stack length, t is the layer thickness, A is the stack cross-sectional area, and u_{ISA} is the dynamic free stroke at voltage V, while $\kappa_C^2 = \frac{d^2}{s\varepsilon} = \frac{k_i u_{ISA}^2}{CV^2}$ is the effective full-stroke electro-mechanical coupling coefficient of the actuator. For magnetoactive actuators, $\kappa_L^2 = \frac{k_i u_{ISA}^2}{LI^2}$ and

$$Z_L(\omega) = i\omega L\left(1 - \kappa_L^2 \frac{\bar{r}(\omega)}{1+\bar{r}(\omega)}\right) \tag{16}$$

The input electrical power can be evaluate as $\frac{1}{2}Y_C V^2$ for capacitive loads, and $\frac{1}{2}Z_L I^2$ for inductive loads, where the frequency dependent Y_C and Z_L are given by Equations (15) and (16), respectively. When the DC bias effects are included, slightly more complicated expressions need to be used, as shown by Giurgiutiu (2000).

5.6 DESIGN OF EFFECTIVE INDUCED-STRAIN ACTUATORS

The design of effective piezo actuators is particularly difficult due to the small displacement generated by these materials. However, the forces that can be generated by a piezo actuator can be very large; are only limited by the inherent stiffness and compressive strength of the piezo material; by its effective area. For most practical applications, displacement amplification of the induced strain displacement is employed. The effective design of the displacement amplifier can "make or break" the practical effectiveness of a piezo actuator. Giurgiutiu *et al.* (1996a,b; 1997a,b) performed extensive studies of the effective design of displacement amplified induced-strain actuators and showed that the most important parameter that needs to be optimized during such a design is the energy extraction coefficient defined as the ratio between the effective mechanical energy delivered

by the actuator and the maximum possible energy that can be delivered by the actuator in the stiffness-match condition. (Giurgiutiu *et al.*, 1997a).

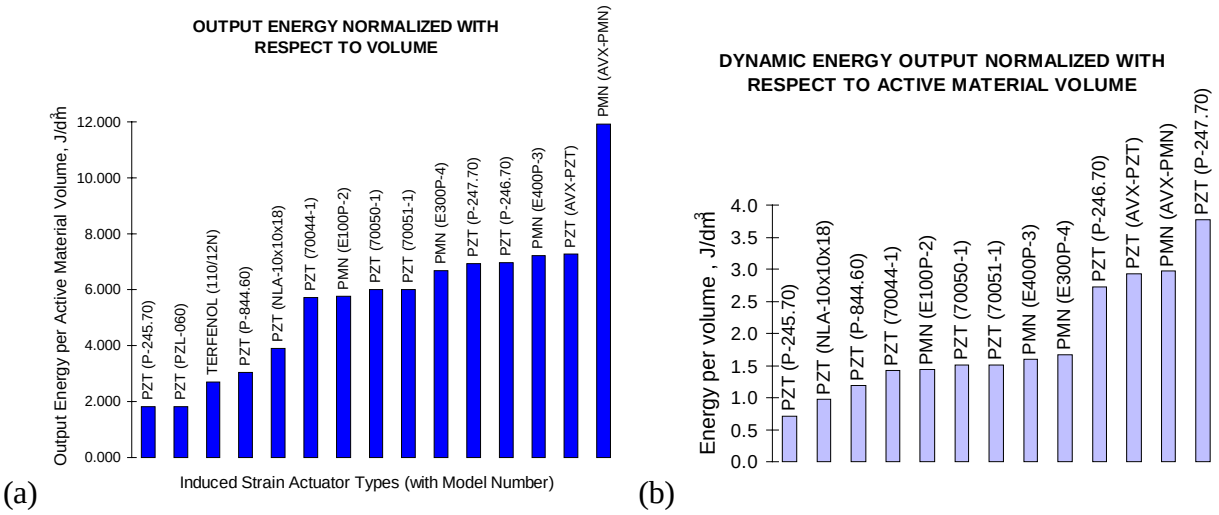

Figure 14: Specific energy output capabilities of a selection of commercially available induced-strain actuators: (a) static operation; (b) dynamic operation.

Of extreme significance in the design of an effective induced-strain actuator is the amount of energy available for performing external mechanical work. Figure 14 presents comparison of the energy density per unit volume for some commercially available induced strain actuators under static and dynamic regimes. Typical energy density values found in these studies (Giurgiutiu *et al.*, 1997b) were placed in the range, 2.71-15.05 J/dm^3 (0.292-1.929 J/kg) under static conditions, and 0.68-3.76 J/dm^3 (0.073-0.482 J/kg) under dynamic conditions. Power densities of up to 23.6 kW/dm^3 (3.0 kW/kg) were predicted at 1 kHz. The overall efficiency of active-material actuation depends, to a great extend, on the efficiency of the entire system that includes the active-material transducer, the displacement amplification mechanisms, and the power supply.

5.7 POWER SUPPLY ISSUES IN INDUCED STRAIN ACTUATION

Since induced-strain actuators can operate in the kHz range, Equation (14), in conjunction with Figure 14, indicates the opportunity for the generation of large output power densities. However, a

number of practical barriers need to be overcome before this can be achieved: (a) the capability of power supply to deliver kVA reactive power; (b) the dissipation of the heat generated in the active material due to internal losses (hysteresis) that can be in the range 5%-10% of the nominal reactive input power; and (c) the electro-mechanical system resonance that sets upper frequency limits.

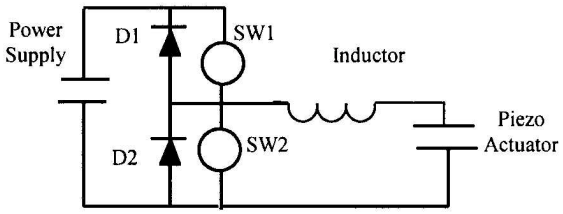

Figure 1 Piezo Switching Amplifier

(a)

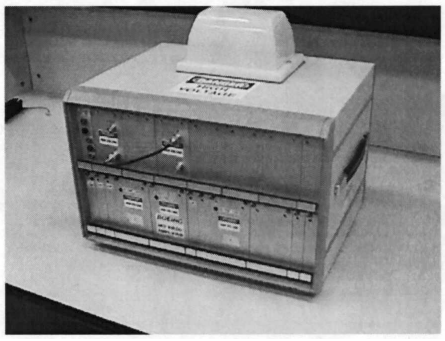

(b)

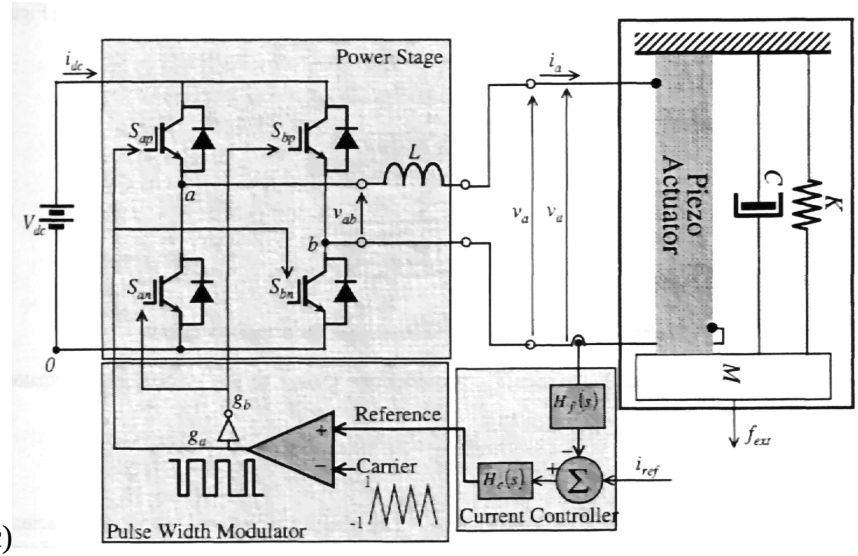

(c)

Figure 15 Power supplies for active material actuators: (a) principle of switching power supplies for high reactive load; (b) a 3000 V switching amplifier (Clingman and Gamble, 2000); (c) schematic of the switching power supply and piezoelectric actuator system (Lidner et al., 2000)

The power supply aspects of induced-strain actuation are currently being address by using specialized power supplies (switching amplifiers) that are able to handle reactive loads much better than conventional linear amplifiers. The switching amplifiers (Figure 15) utilize high frequency pulse width modulation (PWM) principles and solid-state switching technology to drive current in

and out of the capacitive load presented by the induced-strain piezoelectric actuator. In this process, a high-value inductance ballast in utilized (Figure 15a). Lidner *et al.* (2000) have studied the optimal design of such inductive ballast to simultaneously achieve optimal actuator performance and minimum weight (Figure 15c).

The difficulty connected with the electric-supply may seem less severe when using magnetoactive devices, such as Terfenol-D actuators, because they are current driven and require lower voltages at low frequencies. At present, the low-voltage power supply technology is predominant and cheaper than the high-voltage technology, which somehow facilitates the use of magnetostrictive actuators.

Giurgiutiu (2000) studied the effect of adaptive excitation on the current and power requirements, and on the displacement output from a heavy-duty piezoelectric actuator driving a smart structure near the electromechanical resonance (Figure 16). The actuator was assumed to have k_i = 370 kN/mm internal stiffness, C = 5.6 μF internal capacitance, 3.5 kHz resonance, and output displacement $u_m \pm u_a = 22.5 \pm 37.5\ \mu$m when driven by a voltage $V_m \pm V_a = -375 \mp 625$ V. The external mechanical load was assumed to have a matched static stiffness, a mechanical resonance of 30 Hz, and a 1% internal damping. The system was assumed driven by a 1 kVA amplifier, with up to –1000 V voltage and 1A current. As show in Figure 16, the electromechanical system incorporating the structure and the embedded actuator displays an electromechanical resonance at 42.42 Hz. Without adaptive excitation, i.e., under constant voltage supply, the current demands are very large, the actuator experiences a displacement peak that may lead to its destruction, and the required power is excessive. When adaptive excitation was simulated, both the displacement and the current could be kept within bounds, while the power requirements became more manageable and kept within the 1 kVA capability the power amplifier.

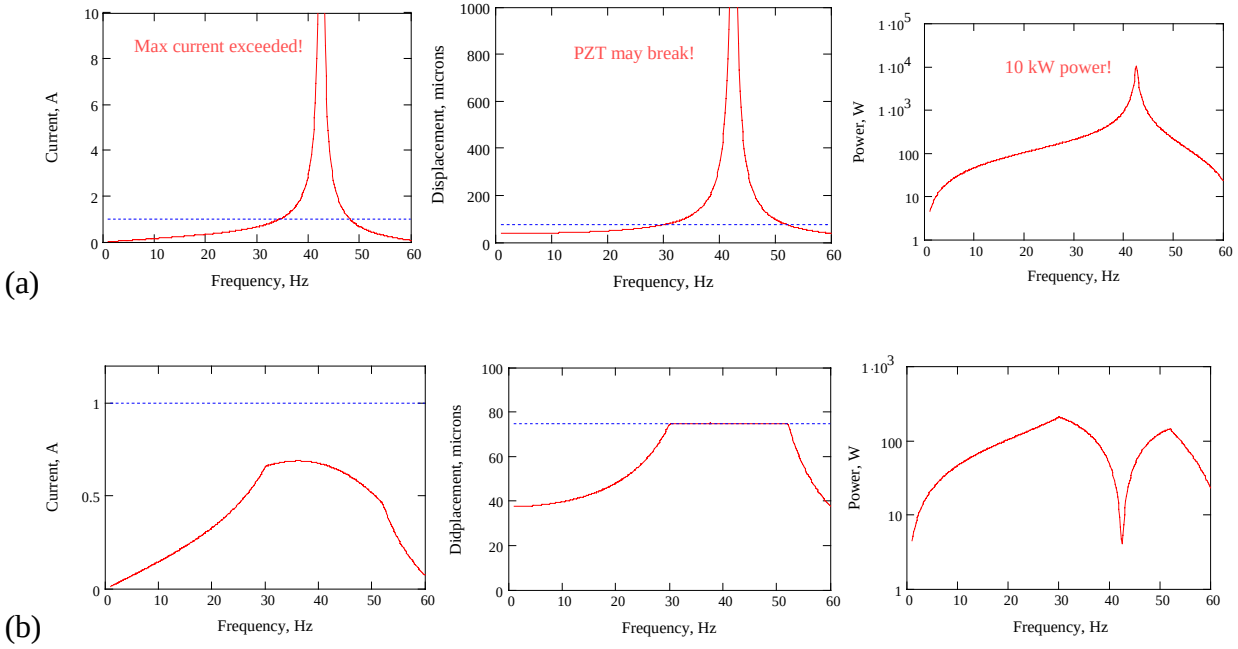

Figure 16 Adaptive excitation of piezoelectric actuators near embedded electromechanical resonance: (a) under constant voltage excitation, the current demands are very large, the actuator may break, and the required power is excessive; (b) with adaptive excitation, both the displacement and the current are kept within bounds, and the power becomes manageable.

6 SMART STRUCTURES

The concept of smart structures has largely evolved by biomimesis and under the influence of Asimov's three laws of robotics. In the biological world, plants and animals alike react to the environment in order to protect their existence, or to acquire the much needed nourishment. For example, the sharp heat from an open flame would instantly make someone to retract his hand. It would also, most probably, make the person shout 'Ouch!". In the engineering world, smart structures are viewed as adaptive systems fitted with sensors, actuators, and command-control processors that could take automatic actions without specific human interventions.

6.1 SENSORY SMART STRUCTURES

Udd (1995) pointed out the sensory smart structures attributes found in even the simplest single-cell micro-organism (Figure 17a). A bridge fitted with smart structure characteristics was conceptualized by Culshaw (1996). Such a "smart" bridge (Figure 17b) would be expected to 'sense' the environment, react accordingly, and 'tell' what is happening by sending alarm signal that announce that strength and safety are diminishing, and appropriate action is needed. In this example, we see a smart structure that is capable of automatic health monitoring, damage detection, and failure prevention.

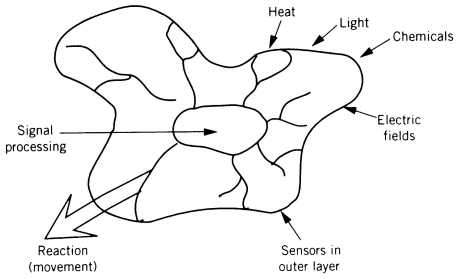

(a)

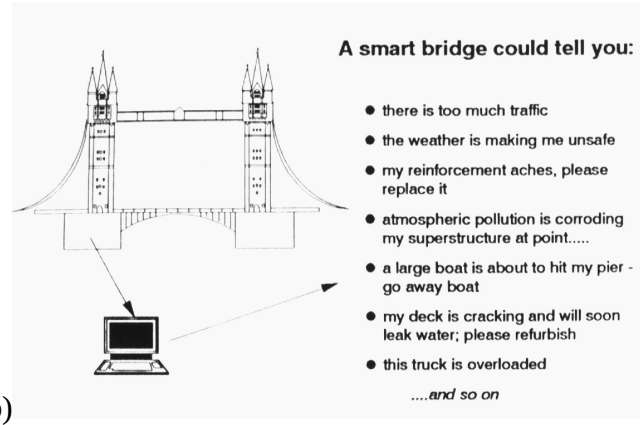

(b)

Figure 17 Sensory smart structures: (a) single cell micro-organism viewed as a sensory smart structure (Udd, 1995); smart structure concept applied to a bridge (after Culshaw, 1996)

6.2 ADAPTIVE ACTUATION SMART STRUCTURES

Another class of smart structure is that fitted with adaptive actuation. Nature offers the ideal example of adaptive actuation. A pair of antagonistic muscles (*musculus biceps brachii* and *musculus triceps brahii*) ensures exact and precise position control during the most difficult maneuvers of our arms. The skeletal muscles of the human arm are attached at a small-displacement high-force positions, well suited for the induced-strain muscle actuation (Figure 18a). Nachtigall (1999) observes that, as a catapulting twitch is performed, the nonlinear skeletal kinematics effects a favorable response during which the distance between the thrown weight and the elbow joint

decreases while the perpendicular distance between the muscle tendon and the joint increases, such that the overall force required in the muscular actuator decreases as the catapulting motion develops.

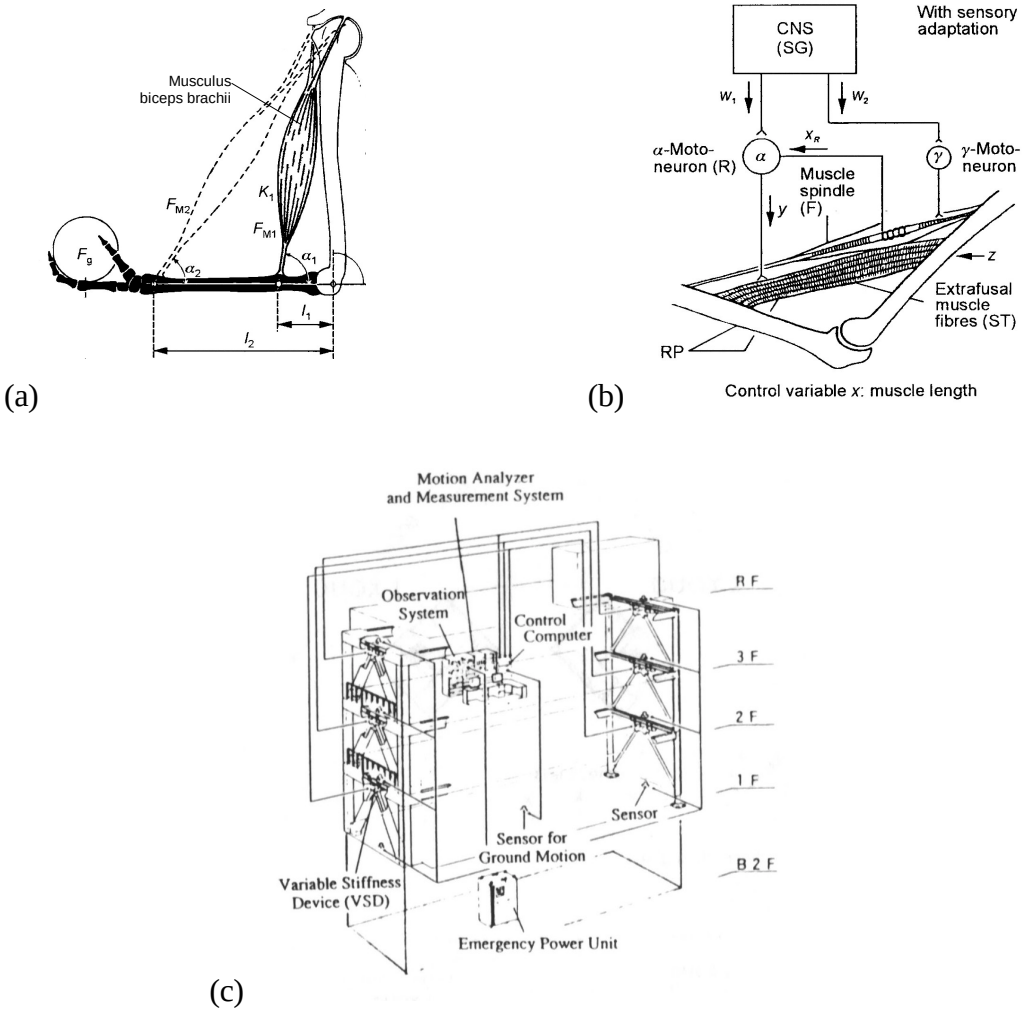

Figure 18 Concepts in adaptive smart structures actuation (a) kinematic of an arm muscle; (b) muscle control system with sensory adaptation (after Nachtingall, 1999); (c) earthquake-resistant variable-stiffness building KaTRI No.21 in service in Tokyo, Japan (after Sakamoto and Kobori, 1994)

In fact, once the weight has been put in motion, the biceps muscle can reduce the contracting signal and even stop before the end of the catapulting motion. In the same time, the antagonistic triceps muscle can start its braking action before the end position has been achieved, such that a smooth transition is achieved. This remarkable feat is accomplished through complex adaptive control

architecture, as depicted in Figure 18b. An engineering building incorporating adaptive structural response is presented in Figure 18c (Sakamoto and Kobori, 1994). This smart structure not only senses and processes the external stimuli, but also takes mechanical action. When the vibration excitation from a gust of wind or earthquake is endangering the structural integrity through excessive resonance response, action is taken in the variable stiffness members such that the structure's natural frequency is shifted and the resonance is avoided. This natural frequency shift achieved through stiffening or relaxing of active structural members resembles the bracing of one's muscles when trying to attain steadiness in a challenging situation. Besides resonance avoidance, smart structures can also attempt to dissipate energy through active and passive mechanisms, or to prevent a nonlinear vibrations or aeroelastic effect from building up through vibration cancellation.

6.3 APPLICATIONS OF SHAPE MEMORY ALLOYS TO VIBRATION CONTROL

Because of its biocompatibility and superior resistance to corrosion, shape memory alloys such as Nitinol have gained wide usage in the medical field as bone plates, artificial joints, orthodontic devices, coronary angioplasty probes, arthroscopic instrumentation, etc. In engineering, these materials have been used as force actuators and robot controls (Funakubo, 1987). They also offer vibration control potentials based on two important principles: (a) the three to four times increase in elastic modulus in the transition from Martensitic to Austenitic phase; (b) the creation of internal stresses; and (c) the dissipation of energy through inelastic hysteretic damping. These effects can be practically realized either as additional components to be retrofitted on existing structures, or as hybrid composite materials containing embedded SMA fibers (Rogers and Robertshaw, 1988).

The increase in elastic modulus is used in the active properties tuning (APT) vibration control method. As SMA wires are activated by heating with electric current or other methods, their modulus increase three fold from 27 GPa to 82 GPa. Depending on the structural architecture and

on how much SMA material is used, this may result in a sizable change in the effective structural stiffness, and a considerable frequency shift away from an unwanted resonance. The activation speed, which depends on the heating rate, is usually sufficient to achieve acceptable structural control. The recovery, however, depends on the rate of cooling, and hence takes place much slower.

The creation of internal stresses is used in the active strain energy tuning (ASET) method. The activation of stretched SMA fibers can make them shrink by 4% to 8% and thus create considerable contractile stress in the support structure. If the SMA fibers are placed inside beams or plates, active frequency control can be readily achieved, since the presence of inplane compressive stresses can considerably change the beams and plates natural frequencies. One ready application of this effect is the avoidance of critical speeds during the run up and run down of high-speed shafts.

6.4 APPLICATIONS OF ELECTRO- AND MAGNETOACTIVE MATERIALS TO VIBRATION CONTROL

Electroactive (PZT and PMN) and magnetoactive (Terfenol-D) actuators can be used as linear actuators to replace conventional devices, or as surface-bonded actuators to induce axial and bending strains in the host structure. In the former case, the strain induced parallel to the field direction is utilized, as, for example, in piezoelectric stacks. In the latter case, the strain induced transverse to the direction of the applied field is used. Linear induced-strain actuator are ideal in retrofit situations when the replacement of a conventional actuator with a "smart" actuator is sought. Surface-bonded actuation is a completely new engineering concept, which is specific to the smart structures world. Bonded electroactive actuator wafers have been used successfully to control the shape of deformable mirrors. In the stack configuration, they have been used for impact dot-matrix printing. Advantages over conventional electromagnetic actuators included order-of-magnitude higher printing speeds, order-or-magnitude lower energy consumption; and reduced noise emissions. A tunable ultrasonic medical probe composed of electroactive elements embedded in a

polymer matrix has also been developed. Electro- and magneto-active materials can be used to enhance structural damping and reduce vibrations. Two mechanisms are available: (a) direct approach, in which the vibration energy is dissipated directly through the electromechanical interaction between the active material and the host structure; (b) indirect approach, in which the active material is used to enhance the damping properties of a conventional damping treatment. The dissipation of vibration energy through the electromechanical interaction of the active materials with the host structure can be achieved either passively or actively. Since the active material is connected to the structure undergoing vibration, the deformation of the active material follows the deformation of the structure. As the structure deforms during vibrations, the active material takes up the strain and transforms it into an oscillatory electrical field.

For passive active-material vibration suppression, the induced electric field is used to drive current into an external resistance thus dissipating the energy through Ohmic heating (Figure 19). In order to dissipate selected frequencies, RCL tuning principles are applied. In active vibration suppression, the active material is used to produce vibration input in anti-phase with the external disturbance, thus resulting in noise and vibrations cancellation. In this case, the energy is dissipated in the heat sink of the driver-amplifier circuit. The active material can be also used to enhance the damping properties of a conventional damping material through the "constraint layer damping effect". Conventional vibration damping treatments utilize the dissipation properties of viscoelastic materials that mainly operate in shear. The shear can be enhanced if, on top of the damping layer, an extra layer of active material is added that deforms in anti-phase with the base

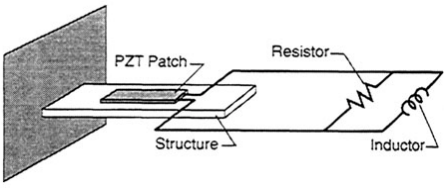

Figure 19 Tuned shunt circuit for vibration control (McGowan *et al.*, 1998)

structure. Thus, the damping layer between the active material layer and the base structure is subjected to a much larger differential shear strain than in the absence of the active layer.

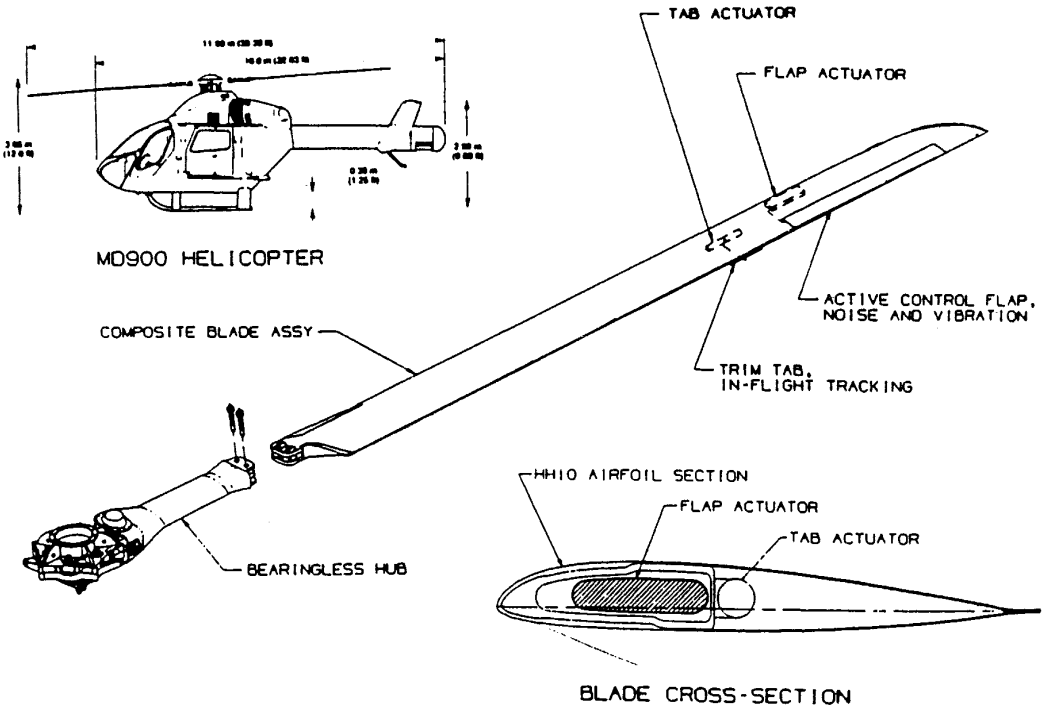

Figure 20 MD 900 helicopter and hingeless blade displaying the planned trim tab for in-flight tracking and active control flap for noise and vibration reduction (Straub and King, 1996).

For illustration, two current aerospace smart structures projects are discussed. One project is aimed at the reduction of noise and vibrations in helicopter rotors (Figure 20). The other project is addressing the buffet vibrations alleviation in a fixed wing aircraft (Figure 21). The smart materials actuation rotor technology (SMART) rotor blade program, under way at Boeing (Mesa), is tasked to test the feasibility of using active materials actuators for rotor blade control to reduce noise and vibrations, improve ride qualities, and extend the service life. The conceptual design of the SMART rotor blade program calls for the simultaneous satisfaction of two important operational requirements: (a) reduction of blade vibration through in-flight rotor track and balance adjustments; and (b) reduction and counteraction of aerodynamically induced noise and vibration through an

actively-controlled aerodynamic surface. The first objective is achieved with a slow-moving trim tab controlled through a bi-directional SMA actuator (Figure 20). The second objective is met with a fast-moving control flap actuated by piezoceramic stacks through a stroke-amplifier.

The second smart structures project to be discussed here relates to aircraft tail buffeting. Tail buffeting is a significant concern for aircraft fatigue and maintenance.The Actively Controlled Response of Buffet Affected Tails (ACROBAT) program studied active materials solutions to resolve the buffet problems of the F/A-18 twin-tail aircraft. A 1/6-scale full-span model was tested in the NASA Langley Transonic Dynamics Tunnel. The portside vertical tail was equipped with surface-bonded piezoelectric wafer actuators, while the starboard vertical tail had an active rudder and other aerodynamic devices. During the wind tunnel tests, constant-gain active control (Figure 21a) was able to reduce power spectral density of the first bending resonance by as much as 60% (Figure 21b).

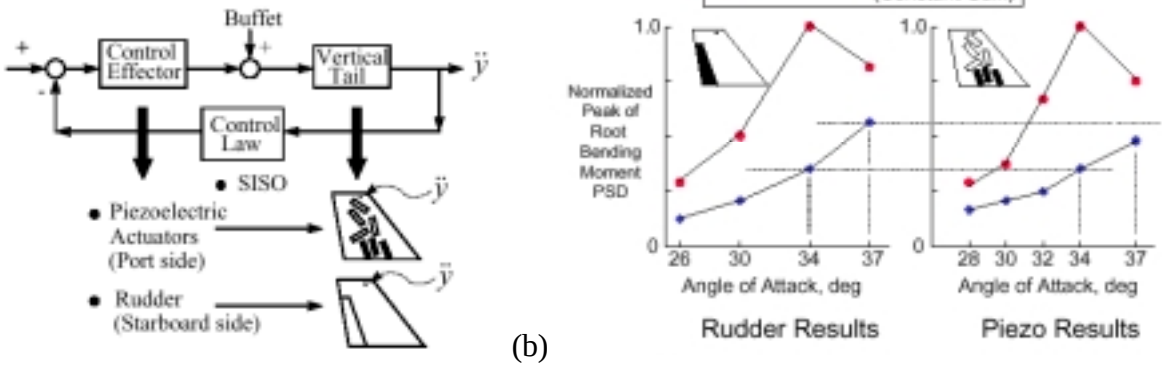

(a) (b)

Figure 21 ACROBAT tail buffet alleviation experiments: (a) single-input single-output (SISO) control law design for active rudder and piezoelectric wafers excitation; (b) power spectrum density (PSD) peak values for the root bending moment at the first bending resonance (Moses 1997).

6.5 ADAPTIVE ALGORITHMS FOR SMART STRUCTURES CONTROL

Implementation of control algorithms in smart structures architecture is subject to attentive scrutiny. Conventional application of classical control algorithms is only the first step in this process. Much better results are obtained if modern adaptive control is use, such that the resulting smart structure can react to changes in the problem-definition parameters. Actual structural designs are very complex, nonlinear in behavior, and subject to load spectra that may be substantially modified during the structures service life. Under such adverse situations, the resulting uncertainty in the controlled plant dynamics is sufficient to make "high-performance goals unreachable and closed-loop instability a likely result" (Clark *et al.*, 1998). To address this problem, at least three adaptive control approaches are advocated: (a) adaptive signal processing methods; (b) model reference adaptive control (MRAC); and (c) self tuning regulators (STR). Though different in details, all three aim at same goal, i.e., to eliminate the effect of variations in disturbance signature and plant dynamics on the smart structure's performance. Many adaptive signal processing algorithms operate in the feedforward path. For example, Fuller (1988) used an acoustic cost function in conjunction with structural inputs in controlling farfield acoustic pressures to achieve aircraft cabin noise cancellation. MRAC and STR are mainly associated with adaptive feedback structural control (see, for example, Astrom and Wittenmark, 1989). Figure 22 illustrates the adaptive feedback and feedforward concepts in an adaptively controlled smart structure. The disturbance input, $u_d(z)$, is fed through the feedforward compensator, $K_{ff}(z)$, and summated with the error signal, $e(z)$, modulated through the feedback compensator, $K_{fb}(z)$, to generate the control signal, $u_c(z)$. The error signal, $e(z)$, is obtained in the classical control fashion by subtracting the resulting output, $y_e(z)$, from the required reference signal, $r(z)$. The blocks $P_{de}(z)$ and $P_{ce}(z)$ represent the plant's response to disturbance and control, respectively. The feedforward compensator, $K_{ff}(z)$, is adaptively modified

in response to trends noticed in the output signal, $y_e(z)$, by the Adaptive Algorithm block that could typically be a least-mean-squares (LMS) method applied to the coefficients of a finite impulse response (FIR) filter. A cost functional incorporating a measure of the output, $y_e(z)$, or a time-averaged gradient (TAG) descent algorithm may be used. Use of hybrid control architecture combines the feedback and feedforward principles to achieve best performance when complex disturbances incorporating both persistent and impulsive components are present.

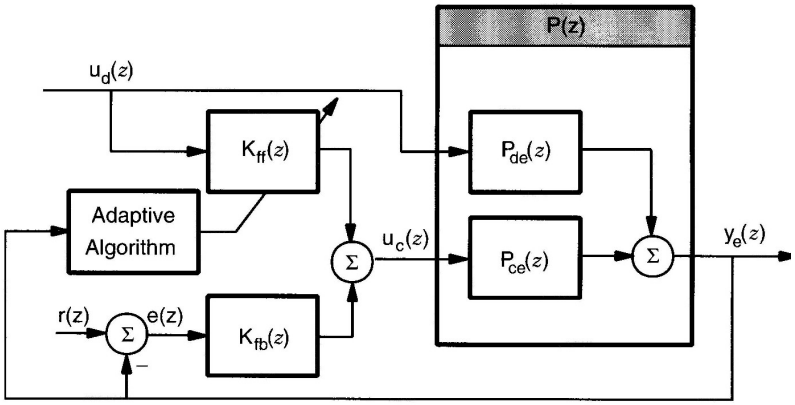

Figure 22 Schematic representation of smart structure with adaptive hybrid control capabilities (after Clark *et al.,* 1998)

7 CONCLUSION

The concepts of induced-strain actuation and smart structures have been reviewed and briefly discussed. Induced-strain actuators are based on active materials that display dimensional changes when energized by electrical, magnetical, or thermal fields. Piezoelectric, electrostrictive, magnetostrictive, and shape memory alloy materials have been presented and analyzed. Of these, piezoelectric (PZT), electrostrictive (PMN), and magnetostrictive (Terfenol-D) materials have been shown to have excellent frequency response (1 to 10 kHz, depending on actuator length), high force (up to 50 kN on current models), but small induced-strain stroke capabilities (typically, 0.1 mm for 0.1% strain on a 100 mm actuator). With this class of induced-strain actuators, displacement amplification devices need always to be incorporated into the application design. In contrast, the shape memory alloy (Nitinol) materials have large induced-strain stroke capabilities (typically, 4 mm for 4% strain on a 100 mm actuator), but low frequency response (< 1 Hz).

The effective implementation of induced strain actuation was discussed and guidelines for achieving optimal energy extraction were presented. As different from conventional actuation techniques, induced-strain actuation can only rely on a limited amount of active stroke, and this has to be carefully managed. We have shown that the stiffness and impedance matching principles can produce the maximum energy extraction from the induced-strain actuator and ensure its transmission into the external application. Details of these principles, together with typical energy density values for various induced-strain actuators have been given. It was found that, for dynamic applications, as much as 3.76 J/dm^3 (0.482 J/kg) could be extracted under dynamic conditions. Power densities of up to 23.6 kW/dm^3 (3.0 kW/kg) were predicted at 1 kHz.

In summary, one can conclude that the potential of smart materials in structural applications has been clearly demonstrated through laboratory research in many institutions around the world. However, the field is still in its infancy and further research and development is required to establish smart materials as reliable, durable, and cost-effective materials for large-scale engineering applications. To promote their use in such engineering applications, the following research directions should be considered. A few that we believe to be most imperative include

(1) The development of smart materials with better performance, together with higher durability and reliability.

(2) The development of new applications that can take full advantage of material ”smartness” through multidisciplinary design optimization.

(3) The integration of various smart materials, or the combination of smart materials with conventional materials, to form functionally integrated smart material systems.

(4) The reduction of production costs for smart materials and systems through economy of scale.

(5) The development of smart materials and concepts applicable to large-scale smart structures applications.

8 REFERENCES

Astrom, K. L. and Wittenmark, B. (1989) *Adaptive Control*, Addison-Wesley, 1989.

Bank, R. (1975) *Shape Memory Effects in Alloys*, p. 537. Plenum, New York,.1975.

Bar-Cohen, Y. and Leary, S. P. (2000) Electroactive Polymers (EAP) Characterization Methods", *Smart Structures and Materials 2000 – Electroactive Polymer Actuators and Devices (EAPAD)*, SPIE Vol. 3987, pp. 12-17.

Barrett, D. J., 1995, "A One-Dimensional Constitutive Model for Shape Memory Alloys", *Journal of Intelligent Material Systems and Structures*, Vol. 6, May 1995, pp. 329-337.

Clark, A. E. (1980) "Magnetostrictive Rare Earth –Fe_2 Compounds", in *Ferromagnetic Materials*, Vol. 1, Wohlfarth. E. P. (Editor), North-Holland, Amsterdam, 1980.

Clark, A. E. (1986) "Magnetostriction in Twinned [112] Crystals of $Tb_{0.27}Dy_{0.73}Fe_2$", *IEEE Transactions Magazine*, MAG-22, pp. 973, 1986.

Clark, A. E. (1992) "High Power Rare Earth Magnetostrictive Materials", In *Proc. Recent Advances in Adaptive and Sensory Materials*, pp. 387-397. Technomic Publishing, Lancaster, PA, 1992. C. A. Rogers and R. C. Rogers Eds.

Clark, R. L.; Saunders, W. R.; and Gibbs, G. (1998) *Adaptive Structures – Dynamics and Control*, Wiley, 1998.

Clingman, D. J.; Gamble, M. (1999) "High Voltage Switching Piezo Drive Amplifier" *SPIE's 6^h International Symposium on Smart Structures and Materials*, 1-5 March 1999, Newport Beach, CA.

Cory, J. S. (1978) "Nitinol Thermodynamic State Surfaces" *J. Energy* **2**, No. 5.

Culshaw, B. (1996) *Smart Structures and Materials*, Artech House Publishers, 1996.

Duerig, T. W.; Melton, K. N.; Stockel, D.; Wayman, C. M. (1990) *Engineering Aspects of Shape Memory Alloys*, Butterworth-Heinemann, 1990.

EDO Corporation, *Piezoelectric Ceramics-Material Specifications, Typical Applications*. Salt Lake City, UT.

Fuller, C. R. (1988) "Analysis of Active Control of Sound Radiation from Elastic Plates by Force Inputs", *Proceedings of Inter-Noise '88*, Avignon, France, Vol. 2, pp. 1061-1064.

Funakubo, H. (1987) *Shape Memory Alloys*. Gordon & Breach, New York,.

Giurgiutiu, V., Craig A. Rogers, C. A. (1997b) "Power and Energy Characteristics of Solid-State Induced-Strain Actuators for Static and Dynamic Applications", *Journal of Intelligent Material Systems and Structures*, Vol. 8, September 1997, pp. 738-750.

Giurgiutiu, V.; (2000) “Mechatronics Aspects of Smart Materials Induced Strain Actuation”, *7th Mechatronics Forum International Conference*, September 6-8 2000, Atlanta, GA, paper #M200-250.

Giurgiutiu, V.; Chaudhry, Z.; Rogers, C. A. (1995) "Engineering Feasibility of Induced-Strain Actuators for Rotor Blade Active Vibration Control", *Journal of Intelligent Material Systems and Structures*, Vol. 6, No. 5, September 1995, Technomic Pub. Co., pp. 583-597.

Giurgiutiu, V.; Chaudhry, Z.; Rogers, C. A. (1996a) "Energy-Based Comparison of Solid-State Induced-Strain Actuators ", *Journal of Intelligent Material Systems and Structures*, Vol. 7, No. 1, January 1996, Technomic Pub. Co., pp. 4-14.

Giurgiutiu, V.; Chaudhry, Z.; Rogers, C. A. (1997a) " Design of Displacement Amplified Induced Strain Actuators for Maximum Energy Output ", ASME *Journal of Mechanical Design* Vol. 119, No. 4, December 1997, pp. 421-524.

Giurgiutiu, V.; Rogers, C. A. (1996b) "Power and Energy Capabilities of Commercially-Available Induced-Strain Actuators under Full-Stroke Dynamic Conditions", *Journal of Intelligent Material Systems and Structures*, Technomic Pub. Co., Vol. 7, No. 6, Nov. 1996, pp. 656-667.

Janocha, H. (1999) *Adaptronics and Smart Structures*, Springer Verlag, 1999.

Lachisserie, Etienne du Tremolet de (1993)*Magnetostriction – Theory and Applications*, CRC Press, 1993.

Lagoudas, D. C., 1995, “Micro-mechanics of Shape Memory Alloys Active Composites and Structures”, 2nd Workshop on Smart Structures and Materials, University of Maryland, September 5-7, 1995.

Liang, C.; Rogers, C. A. (1990) “A One-Dimensional Thermomechanical Constitutive Relation of Shape Memory Materials”, *J. Intell. Mater. Syst. Struct.* **1**(2), 207-234.

Lindner, D. K.; Chandrasekaran, S. (2000) “Optimization of Switching Amplifiers for Piezoelectric Actuators”, *SPIE’s 7th International Symposium on Smart Structures and Materials*, 5-9 March 2000, Newport Beach, CA, SPIE Vol. 3991, pp 418-429.

Moses, R. W. (1997b) “Active Vertical Tail Buffeting Alleviation on a Twin-Tail Fighter Configuration in a Wind Tunnel”, *CEAS International Forum on Aeroelasticity and Structural Dynamics 1997*, Rome, Italy, June 17-20, 1997.

Muller, I. (1979) “A Model for a Body with Shape Memory”, *Arch. Ration. Mech. Anal.* **70**, 61-77.

Nachtigall, W. (1999) “Adaptronic Systems in Biology and Medicine” in *Adaptronics and Smart Structures*, H. Janocha (Ed.), Springer, 1999.

Paine, J. S. N., Rogers, C. A., 1994, “Low Velocity Perforating Impact Response of Shape Memory Alloy Hybrid Composite Materials”, *ASME Adaptive Structures and Composite Materials: Analysis and Applications*, AD-Vol. 45, pp. 75-84.

Paine, J. S. N., Rogers, C. A., 1995, "High Velocity Impact Response of Composites with Surface Bonded Nitinol-SMA Hybrid Layers", *Proceedings of the 36th AIAA/ASME/ASCE/AHS/ASC Structures, Structural Dynamics, and Materials Conference*, New Orleans, April 9-12, 1995, Paper # AIAA-95-1409-CP, pp. 2084-2094.

Park, S-.E., and Shrout T. R., "Ultrahigh strain and piezoelectric behavior in relaxor ferroelectric single crystals", Journal of Applied Physics, Vol. 4, No. 82, pp. 1804-1811, 1997

Piezo Systems, Inc., *Piezoelectric Motor/Actuator Kit Manual*. Piezo Systems, Inc., Cambridge, MA.

Rogers, C. A.; Robertshaw, H. H. (1988) "Shape Memory Alloy Reinforced Composites", *Eng. Sci. Repr*. **ESP25.88027**.

Sakamoto M. and Kobori, T. (1994) "Control Effect During Actual Earthquake and Strong Winds of Active Structural Response Control of Buildings", *5th International Conference on Adaptive Structures*, Sendai, Japan, December 1994.

Straub, F. K.; King, R. J. (1996) "Application of Smart Materials to Control of a Helicopter Rotor", *SPIE Symposium on Smart Structures and Materials*, San Diego, CA, February 26-29, 1996.

Tanaka K.; Nagaki, S. (1982) "A Thermomechanical Description of Materials with Internal Variables in the Process of Phase Transformation", *Ing. Arch*. **51**, 287-299.

Tanaka, K.; R. Iwasaki (1985) "A Phenomenological Theory of Transformation Superplasticity", *Engineering Fracture Mechanics*, **21**(4), pp. 709-720.

Udd, E. (1995) *Fiber Optic Smart Structures*, Wiley, 1995.